# Seasonal variations in the sources of natural and anthropogenic lead deposited at the East Rongbuk Glacier in the high-altitude Himalayas

Laurie Burn-Nunes [a,*], Paul Vallelonga [b], Khanghyun Lee [c], Sungmin Hong [d], Graeme Burton [a], Shugui Hou [e], Andrew Moy [f,g], Ross Edwards [a,1], Robert Loss [a], Kevin Rosman [a]

[a] Department of Imaging and Applied Physics, Curtin University, GPO Box U 1987, Perth 6845, Western Australia, Australia
[b] Centre for Ice and Climate, Niels Bohr Institute, University of Copenhagen, Juliane Maries Vej 30, DK-2100 Copenhagen Ø, Denmark
[c] Environmental Measurement and Analysis Center, National Institute of Environmental Research, Environmental Research Complex, Kyungseo-dong, Seo-gu, Incheon 404-170, Republic of Korea
[d] Department of Ocean Sciences, Inha University, 100 Inha-ro, Nam-gu, Incheon 402-751, Republic of Korea
[e] Key Laboratory of Coast and Island development of Ministry of Education, School of Geographic and Oceanographic Sciences, Nanjing University, Nanjing 210093, China
[f] Department of the Environment, Australian Antarctic Division, Channel Highway, Kingston 7050, Tasmania, Australia
[g] Antarctic Climate and Ecosystems Cooperative Research Centre, University of Tasmania, Private Bag 80, Hobart 7001, Tasmania, Australia

## HIGHLIGHTS

- Pb isotopes in ice and snow show seasonality in Mt Everest atmospheric chemistry.
- Local (Himalayan) mineral dust inputs are present year round.
- Regional and long-range mineral dust inputs are evident during non-monsoon times.
- Snow samples indicate increased anthropogenic inputs during non-monsoon times.
- Anthropogenic inputs are linked with Indian, South Asian and Central Asian sources.

## ARTICLE INFO

## ABSTRACT

Lead (Pb) isotopic compositions and concentrations, and barium (Ba) and indium (In) concentrations have been analysed at sub-annual resolution in three sections from a <110 m ice core dated to the 18th and 20th centuries, as well as snow pit samples dated to 2004/2005, recovered from the East Rongbuk Glacier in the high-altitude Himalayas. Ice core sections indicate that atmospheric chemistry prior to ~1953 was controlled by mineral dust inputs, with no discernible volcanic or anthropogenic contributions. Eighteenth century monsoon ice core chemistry is indicative of dominant contributions from local Himalayan sources; non-monsoon ice core chemistry is linked to contributions from local (Himalayan), regional (Indian/Thar Desert) and long-range (North Africa, Central Asia) sources. Twentieth century monsoon and non-monsoon ice core data demonstrate similar seasonal sources of mineral dust, however with a transition to less-radiogenic isotopic signatures that suggests local and regional climate/environmental change. The snow pit record demonstrates natural and anthropogenic contributions during both seasons, with increased anthropogenic influence during non-monsoon times. Monsoon anthropogenic inputs are most likely sourced to South/South-East Asia and/or India, whereas non-monsoon anthropogenic inputs are most likely sourced to India and Central Asia.

© 2014 Elsevier B.V. All rights reserved.

## 1. Introduction

The high-altitude Himalayas are a unique region to study atmospheric chemistry as the region is impacted by both low-altitude regionally-sourced winds and upper tropospheric hemispherically-sourced winds, both of which are associated with the annual cycle in the Asian monsoon

(Barry, 1981). Regional precipitation is dominated by the Asian monsoon, with high rates of precipitation during the monsoon season (June to September) and drier conditions during the non-monsoon season (October to May). Snow and ice recovered from Mount Everest has demonstrated well-preserved seasonality in major ions and trace metals, with higher concentrations during the non-monsoon season (e.g. Kang et al., 2004, 2007; Lee et al., 2008; Duan et al., 2009; Zhang et al., 2009; Liu et al., 2010). Early provenance studies linked non-monsoon mineral dust to arid/semi-arid regions in northern China (Kang et al., 2001 and references therein), however such southward pathways of mineral dust were later

shown to be unlikely (Sun et al., 2001; Tsai et al., 2008); similar conclusions were reached on the southerly transport of Tibetan Plateau dust (Zhang et al., 2009). Recently, local Himalayan exposed rock areas, regional deserts in northern India and Central Asia, and long-range desert regions such as the Sahara and Arabian Peninsula have been suggested as the most likely non-monsoon mineral dust source regions, with local mineral dust sources suggested for monsoon dust deposition (see Kang et al., 2007; Ming et al., 2007; Kaspari et al., 2009a; Liu et al., 2010; Lee et al., 2011 and references therein). These results are supported by back trajectory analyses (Cong et al., 2009; Zhang et al., 2009; Kaspari et al., 2009a; Liu et al., 2010).

Investigations of heavy metal deposition in the Mount Everest region are relatively recent and have produced contrasting results. Kang et al. (2007) and Zhang et al. (2008, 2009) found little evidence of anthropogenic influence on the Mount Everest atmospheric environment in recent decades which is in contrast to the results discussed by Lee et al. (2008) and Duan et al. (2009). Recently, Lee et al. (2011) and Hong et al. (2012) reported trace element concentrations and lead (Pb) isotopic compositions during the past 800 years from an East Rongbuk Glacier (ERG) ice core, demonstrating the presence of anthropogenic impurities in Mount Everest ice and speculating on pollution sources within South Asia (India as well as the possibility of Bangladesh and Nepal).

Whilst Lee et al. (2011) and Hong et al. (2012) both present an exhaustive Pb isotopic study of high-altitude Himalayan ice, they were only able to quantitatively examine sources based on annual averages. As a result, the seasonal nature of deposition of impurities, and the differing sources and transport patterns associated with the monsoon climate, could not be defined. Consequently, to investigate seasonal variability in the sources of natural and anthropogenic impurities impacting on the East Rongbuk Glacier environment, we have determined lead (Pb), barium (Ba) and indium (In) concentrations and Pb isotopes in three ice core sections dated to the 18th and 20th centuries and sampled at monthly to quarterly resolution, as well as a series of snow pit samples, previously discussed by Lee et al. (2008). Barium and indium are important respective indicators of mineral dust levels

(Patterson and Settle, 1987) and volcanic emissions (Hinkley and Matsumoto, 2007 and references therein). This study provides the first detailed investigation of the natural and anthropogenic sources of deposited impurities and provides more definitive evidence of the atmospheric transport paths that lead to this deposition in the high-altitude Himalayan region.

## 2. Materials and methods

### 2.1. Samples

#### 2.1.1. Ice Cores

In 2002, a 108.83 m ice core was recovered to bedrock from the col of the East Rongbuk Glacier (henceforth referred to as "ERG", 28.038°N, 86.968°E; 6518 m a.s.l., Fig. 1), on the north-east ridge of Mount Everest, using an electromechanical drill in a dry hole. Hou et al. (2007) have described the ice coring site to be located at the periphery of a percolation zone where annual layers are made up of alternating summer percolation and winter dry snow strata. In a recent study, Wong et al. (2013) investigated in detail the impact of surface melt and subsequent percolation on the preservation of ice core records and found particle-bound elements to remain relatively immobile. Therefore Pb (and Ba, In), all of which are particle-bound, should not be significantly mobilized from surface melt at the ERG ice coring site. This, in addition to the seasonality in major ions and trace elements that has been demonstrated in the ERG ice core (e.g. Kang et al., 2007; Kaspari et al., 2009b) and the lack of observed melt layers in sampled snow from the same site (Lee et al., 2008) implies that post-depositional processes are not likely to have significantly impacted on the ERG records that are presented here.

Kaspari et al. (2007) have dated the ERG core to 1534 AD, at a depth of 98 m, based on seasonal signals preserved in hydrogen isotopes ($\delta D$) and soluble ions in the ERG ice, verifying the timescale by identifying large bismuth horizons attributed to volcanoes. Based on this annual layer dating, the three ice core sections reported here from depths 35.42–35.78 m, 48.25–48.51 m and 72.16–72.45 m have been dated to 1952.7–1952.0 ($\pm$0.1 years), 1913.6–1912.0 ($\pm$0.6 years) and
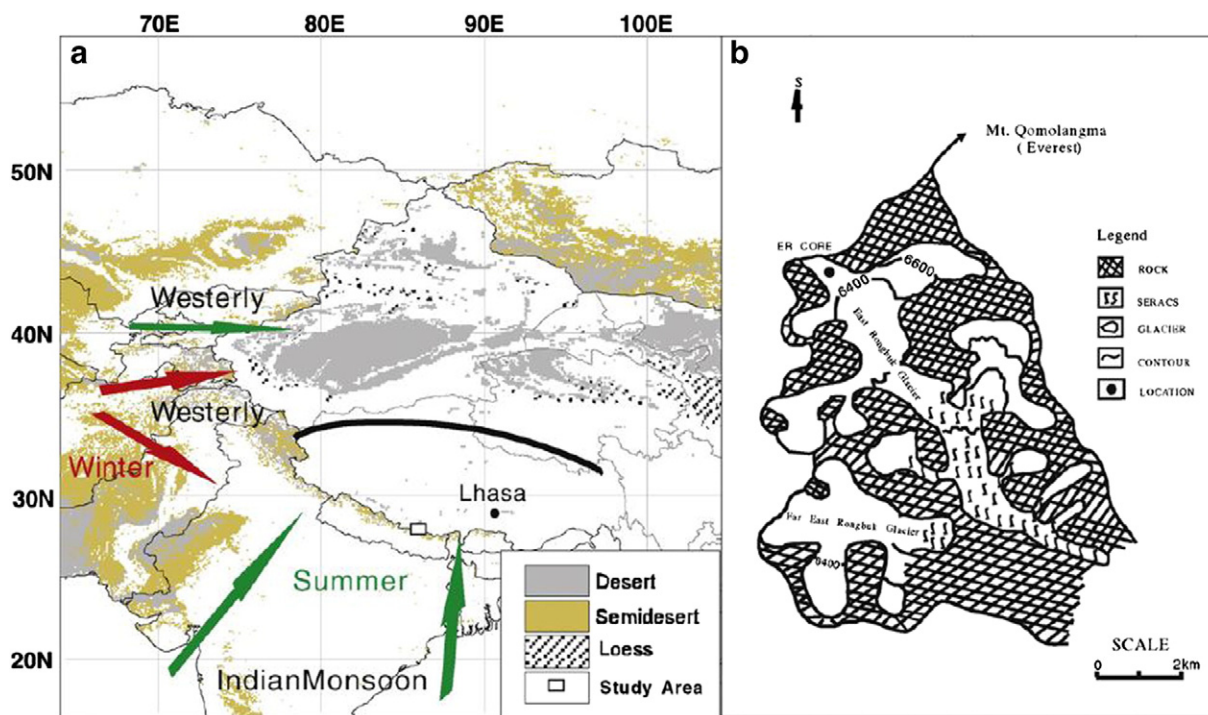


**Fig. 1.** Location of the East Rongbuk Glacier (ERG) ice core drilling site in the central/eastern Himalayas. In the right image, white areas are snow and ice, and grey areas are rock. General summer and winter circulations are also shown. Note: Qomolangma is an alternate name for Mount Everest.
From Lee et al. (2008), permission obtained from Elsevier Limited.

1775.5–1773.2 ($\pm$ 2.2 years) respectively where dating uncertainties have been calculated based on data presented by Kaspari et al. (2007) (Auxiliary Material).

### 2.1.2. Surface Snow

In September 2005, a shallow snow pit was excavated at the East Rongbuk Glacier and a continuous series of 42 samples were collected from the snow surface, at 5 cm intervals, to a depth of 2.1 m (see details in Lee et al., 2008). Samples were dated by combining oxygen isotopes, major ions and aluminium content. The top 115 cm of the snow pit was found to be associated with 2005 summer monsoon deposition, and the bottom 115–210 cm to preceding non-monsoon deposition during the autumn of 2004.

### 2.2. Processing

The three ERG ice core sections discussed here were decontaminated and sampled inside a −10 °C cold clean room at Curtin University, following procedures discussed in detail by Burn et al. (2009). Transverse sectioning was accomplished using a clean mechanized stainless steel circular saw blade, achieving sample resolutions of 4 cm (~1952 AD section) down to 1 cm (~1774 AD section). Decontaminated samples were collected in a low-density polyethylene (LDPE) box and transferred to a LDPE "melt vial" for storage. Since only eight saw blades were available, blades were re-cleaned during the slicing process by transferring them to the adjoining laboratory maintained at ~22 °C where they were immersed in warm one-molar nitric acid (1 M $HNO_3$), followed by ultra-pure water (UPW), then allowed to dry before reuse. Collected samples were then stored frozen until required for analysis. Burn et al. (2009) found this procedure to be low in contamination with a total blank added to each inner core slice of 0.2 $\pm$ 2 pg Pb with $^{206}Pb/^{207}Pb$ and $^{208}Pb/^{207}Pb$ ratios of 1.16 $\pm$ 0.12 and 2.35 $\pm$ 0.16, and Ba and In amounts of 1.5 $\pm$ 0.4 pg and 0.6 $\pm$ 2.0 fg respectively.

For the snow pit samples, 42 aliquots (approximately 30 mL) were transferred from the Korean Polar Research Institute (KOPRI) to Curtin University. These samples did not require any further processing.

Various studies have shown Pb, Ba and In concentrations in small volumes of glacial ice to be sufficiently low to allow their direct analysis by Thermal Ionisation Mass Spectrometry (e.g. Rosman et al., 2000; Burton et al., 2007; Burn-Nunes et al., 2011 and references therein). Therefore, for both the ice core and the snow pit samples analysed in this study, ion exchange chemistry was not necessary and melted aliquots of each sample ranging from 2 to 10 g were transferred directly to a preconditioned 15 mL Perfluoroalkoxy (PFA) beaker containing 10 μL of nitric acid ($HNO_3$), 20 μL of hydrofluoric acid (HF), and 4 μL of dilute phosphoric acid ($H_3PO_4$, approximately 5% by weight). To enable the amounts of Pb, Ba and In in the samples to be accurately determined by Isotope Dilution Mass Spectrometry (IDMS), 10 μL of a calibrated mixed tracer solution containing accurately determined amounts of the enriched isotopes $^{205}Pb$, $^{137}Ba$, and $^{113}In$ was added to each sample (Matsumoto and Hinkley, 1997; Jimi et al., 2008). The mixture was then evaporated to dryness inside a polytetrafluoroethylene (PTFE) chamber under an infrared lamp, as described by Chisholm et al. (1995). The evaporated residue was then transferred in a droplet of a silicic acid silica gel/phosphoric acid ionisation enhancer to an acid-cleaned zone-refined rhenium mass spectrometer filament and dried by passing an electric current through the filament. One to two sample preparation blanks and one reference sample containing approximately 50 pg of NIST 981 Pb Isotopic Standard Reference Material were also analysed with each batch ('turret') of 18 samples. Sample preparation blanks averaged 0.4 pg Pb, 6 pg Ba and 4 fg In over the course of all measurements; blank Pb isotopic compositions were assessed for each individual turret.

### 2.3. Mass spectrometry

Lead (Pb), Ba, and In concentrations and ratios in the ice core samples were analysed using a combination of a 21-sample turret ThermoFinnigan TRITON Isotope Ratio Thermal Ionisation Mass Spectrometer (IR-TIMS, Bremen, Germany), and a 16-sample turret VG 354 Fisons Instruments TIMS. Snow pit samples were analysed using the ThermoFinnigan TRITON TIMS. Both instruments feature a 90° magnetic sector, with a 23 cm radius on the TRITON and a 27 cm radius on the VG 354. TRITON ion beams were measured using a secondary electron multiplier (SEM) operated in pulse counting mode; VG ion beams were measured using a Daly collector operated in analogue mode. The linear mass bias for each instrument, introduced into the isotopic ratios by evaporation of the sample and other factors, was determined by regular measurement of the NIST SRM981 standard and evaluated to be 0.26 $\pm$ 0.07% per mass unit for the TRITON and 0.25 $\pm$ 0.06% per mass unit for the VG 354 measurement. Measurements of NIST SRM981 on the TRITON also showed that apart from isotopic fractionation there was a bias (low) of 0.2% in the $^{208}Pb$ isotope abundance, which is smaller than the precisions reported here and so does not affect any of the conclusions.

For oxygen isotope ($\delta^{18}O$) composition measurements of the ice core samples, sub-samples (1 mL) were equilibrated with a reference carbon dioxide ($CO_2$) gas at 25 °C using a VG Isoprep-18 equilibration bench at the University of Tasmania. The oxygen isotope ratio of equilibrated $CO_2$ was measured on a VG Isogas Isoprep-18 Stable Isotope Ratio Analysis (SIRA) mass spectrometer. The $\delta^{18}O$ values are expressed as per mil (‰) relative to the Vienna Standard Mean Oceanic Water (V-SMOW) standard. The standard deviation of the $\delta^{18}O$ values for repeated measurements of laboratory reference water samples was <0.07‰.

### 2.4. Corrections made to ice core data

All ice core and snow pit data have been corrected for contamination added during processing and sample preparation. In the case of the ice core data, contamination was found to originate from three sources: (1) ice core processing (decontamination and inner core slicing); (2) sample melt vials; and (3) sample preparation. Contributions associated with (1) and (3) have been quantified in Section 2.2. For (2), the melt vial blank was assessed and found to be 0.010 $\pm$ 0.002 pg g$^{-1}$, 0.03 $\pm$ 0.02 pg g$^{-1}$ and 0.01 $\pm$ 0.06 fg g$^{-1}$ for Pb, Ba and In respectively, with $^{206}Pb/^{207}Pb$, $^{208}Pb/^{207}Pb$ and $^{206}Pb/^{204}Pb$ ratios of 1.16 $\pm$ 0.03, 2.41 $\pm$ 0.06 and 17.2 $\pm$ 1.7 respectively.

In the case of snow pit data, contamination was found to come from two sources: (1) sample storage bottles; and (2) sample preparation. The latter has been quantified in Section 2.2; contributions from (1) were assessed and found to be negligible for Ba and In concentrations, and the Pb concentration and $^{206}Pb/^{207}Pb$, $^{208}Pb/^{207}Pb$ and $^{206}Pb/^{204}Pb$ ratios were found to be 0.03 $\pm$ 0.01 pg g$^{-1}$ and 1.12 $\pm$ 0.01, 2.40 $\pm$ 0.01 and 17.2 $\pm$ 0.3 respectively.

Following elemental and isotopic correction for all blanks, sample Pb isotopic data were corrected for fractionation associated with the TIMS isotopic measurement, which has been quantified in Section 2.3.

### 2.5. Seasonal apportionment of ice core data

It is common practice to differentiate Himalayan snow and ice strata by season (monsoon and non-monsoon) based on parameters such as soluble ions, trace elements, mineral dust proxies and oxygen isotope ratios (Wake and Stievenard, 1995; Kang et al., 2000, 2002, 2007; Zhang et al., 2005; Kaspari et al., 2008; Lee et al., 2008). In this study, we have utilised oxygen isotopes and Ba concentrations, as proxies for seasonality, to assign monsoon and non-monsoon seasons to ice core data, as shown in Fig. 2 and listed in Table 1. However, given the strong [Pearson] correlations that exist between Ba–Pb and Ba–In in this study (R = 0.97 and R = 0.96 respectively), this attribution strongly biases
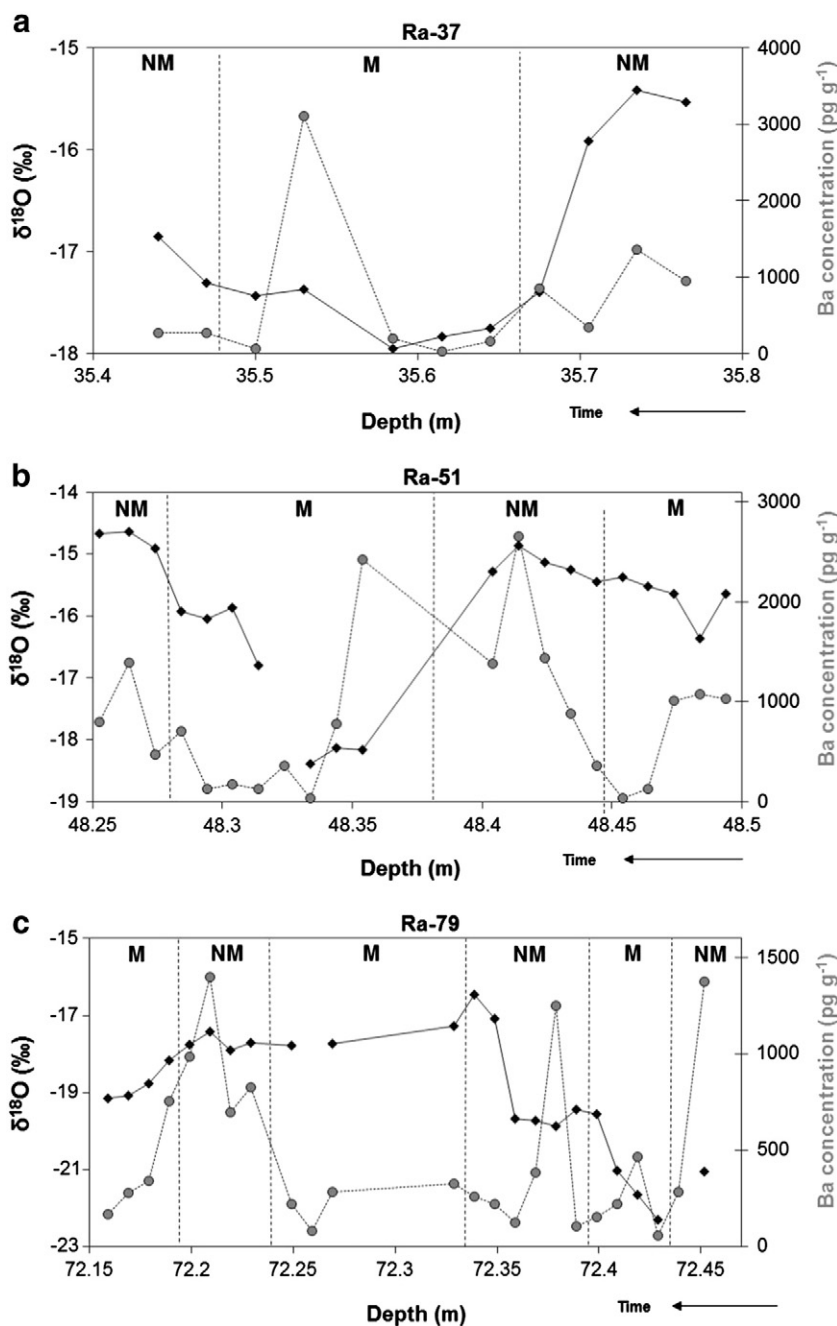
**Fig. 2.** Differentiation of monsoon (M) and non-monsoon (NM) seasons based on measured oxygen isotopes ($\delta^{18}O$) and Ba concentrations in: (a) Ra-37 (~1952 AD); (b) Ra-51 (~1912 AD); and (c) Ra-79 (~1774 AD) ice core sections. Black diamonds indicate $\delta^{18}O$ values (per mil, ‰) and grey circles indicate Ba concentrations (pg g$^{-1}$).

and hence prevents any interpretations of Pb (and In) in terms of seasonality. In contrast, correlations between Ba and Pb isotopic ratios are weaker. Therefore, whilst the two parameters might not be entirely independent, we deem Pb isotopic ratios to be decoupled enough to enable their utilisation for interpreting seasonal patterns.

## 3. Results and discussion

### 3.1. Ice cores

Fully corrected (processing/preparation blanks, instrumental fractionation) inner ice core data are given in Table 1. The reliability of the measured data was assessed from profiles of Pb concentrations and $^{206}Pb/^{207}Pb$ ratios following the guidelines presented by Burn et al. (2009), whereby a plateau in Pb concentrations and $^{206}Pb/^{207}Pb$ ratios

must be achieved from the innermost decontaminated layers to the average of the inner core slices. Such plateaus were observed for all decontaminated ice core sections, demonstrating that external contamination was not present in the inner core sections (see Supplementary Material).

Characteristics of the data set are discussed below where "Ra-79", "Ra-51" and "Ra-37" refer to ice core sections dated to ~1774 AD (18th century), ~1912 AD and ~1952 AD (20th century) respectively.

### 3.1.1. Oxygen isotopes

Variability in oxygen isotope composition ($\delta^{18}O$) is evident in each of the three ice core sections. The annual cycle in $\delta^{18}O$ in southern Tibetan Plateau precipitation is well established, characterised by: depleted values from mid to late summer; increasing values from autumn to winter; and increasing values from winter to spring reaching the least

**Table 1**
Analysed Mount Everest ice core data.

| Core samples | | | δ¹⁸O | Season | Concentrations | | | | | | | | Lead isotopic ratios | | | | | |
|---|---|---|---|---|---|---|---|---|---|---|---|---|---|---|---|---|---|---|
| Core section | Mid depth (m) | Age (years AD) | | | Pb (pg g⁻¹) | ± | Ba (pg g⁻¹) | ± | In (fg g⁻¹) | ± | Pb/Ba | ± | ²⁰⁶Pb/²⁰⁷Pb | ± | ²⁰⁸Pb/²⁰⁷Pb | ± | ²⁰⁶Pb/²⁰⁴Pb | ± |
| Ra-37 | 35.440 | 1952.70 | −16.85 | NM | 16.5 | 0.7 | 274.5 | 10.9 | 54.4 | 2.6 | 0.060 | 0.003 | 1.200 | 0.001 | 2.496 | 0.002 | 18.9 | 0.1 |
| | 35.470 | 1952.64 | −17.30 | NM | 35.2 | 1.4 | 268.3 | 10.5 | 41.6 | 2.2 | 0.131 | 0.007 | 1.210 | 0.002 | 2.482 | 0.003 | 19.3 | 0.1 |
| | 35.500 | 1952.58 | −17.43 | M | 6.2 | 0.3 | 61.5 | 2.8 | 3.5 | 0.8 | 0.101 | 0.006 | 1.181 | 0.002 | 2.478 | 0.004 | 18.7 | 0.2 |
| | 35.530 | 1952.51 | −17.37 | M | 206.1 | 8.4 | 3106.1 | 140.1 | 463.0 | 19.2 | 0.066 | 0.004 | 1.205 | 0.001 | 2.497 | 0.002 | 19.0 | 0.1 |
| | 35.585 | 1952.40 | −17.95 | M | 7.5 | 0.3 | 192.6 | 7.8 | 14.0 | 1.0 | 0.039 | 0.002 | 1.194 | 0.002 | 2.499 | 0.004 | 18.8 | 0.1 |
| | 35.615 | 1952.34 | −17.84 | M | 3.5 | 0.2 | 31.2 | 1.6 | 0.0 | 0.5 | 0.112 | 0.008 | 1.189 | 0.002 | 2.499 | 0.006 | 18.6 | 0.4 |
| | 35.645 | 1952.27 | −17.75 | M | 9.1 | 0.4 | 158.3 | 6.5 | 15.2 | 1.2 | 0.057 | 0.003 | 1.199 | 0.002 | 2.500 | 0.003 | 18.9 | 0.2 |
| | 35.675 | 1952.21 | −17.39 | NM | 45.3 | 1.8 | 855.2 | 65.6 | 121.9 | 5.4 | 0.053 | 0.005 | 1.213 | 0.002 | 2.501 | 0.002 | 19.2 | 0.1 |
| | 35.705 | 1952.15 | −15.92 | NM | 39.4 | 1.6 | 342.3 | 15.1 | 39.7 | 2.2 | 0.115 | 0.007 | 1.203 | 0.001 | 2.500 | 0.002 | 19.1 | 0.1 |
| | 35.735 | 1952.08 | −15.42 | NM | 85.9 | 3.6 | 1362.7 | 56.4 | 234.1 | 10.2 | 0.063 | 0.004 | 1.197 | 0.002 | 2.495 | 0.004 | 19.0 | 0.3 |
| | 35.765 | 1952.02 | −15.54 | NM | 76.4 | 3.0 | 954.1 | 38.1 | 155.0 | 6.6 | 0.080 | 0.004 | 1.198 | 0.003 | 2.491 | 0.005 | 18.9 | 0.1 |
| Ra-51 | 48.253 | 1913.58 | −14.66 | NM | 70.6 | 3.0 | 799.8 | 35.6 | 163.9 | 7.3 | 0.088 | 0.005 | 1.194 | 0.001 | 2.482 | 0.003 | 18.8 | 0.1 |
| | 48.264 | 1913.49 | −14.64 | NM | 90.3 | 3.6 | 1396.7 | 61.2 | 247.5 | 10.2 | 0.065 | 0.004 | 1.204 | 0.002 | 2.494 | 0.003 | 19.0 | 0.1 |
| | 48.274 | 1913.43 | −14.91 | NM | 33.1 | 1.3 | 470.9 | 19.3 | 74.4 | 3.2 | 0.070 | 0.004 | 1.197 | 0.002 | 2.488 | 0.003 | 18.8 | 0.1 |
| | 48.284 | 1913.36 | −15.93 | M | 25.7 | 1.1 | 704.0 | 29.5 | 104.9 | 4.6 | 0.036 | 0.002 | 1.199 | 0.002 | 2.499 | 0.003 | 18.9 | 0.1 |
| | 48.294 | 1913.29 | −16.05 | M | 13.5 | 0.6 | 128.1 | 6.0 | 14.5 | 1.2 | 0.105 | 0.007 | 1.195 | 0.003 | 2.488 | 0.005 | 18.8 | 0.2 |
| | 48.304 | 1913.22 | −15.87 | M | 19.6 | 0.8 | 176.2 | 8.3 | 17.3 | 1.1 | 0.111 | 0.007 | 1.187 | 0.003 | 2.483 | 0.004 | 18.7 | 0.2 |
| | 48.314 | 1913.16 | −16.79 | M | 6.3 | 0.3 | 130.4 | 6.7 | 14.3 | 1.3 | 0.049 | 0.003 | 1.191 | 0.003 | 2.483 | 0.008 | 18.9 | 0.4 |
| | 48.324 | 1913.09 | | M | 11.2 | 0.6 | 364.5 | 18.5 | 41.3 | 2.8 | 0.031 | 0.002 | 1.182 | 0.004 | 2.476 | 0.010 | 18.5 | 0.5 |
| | 48.334 | 1913.02 | −18.39 | M | 2.1 | 0.1 | 30.2 | 2.2 | 2.8 | 0.6 | 0.069 | 0.007 | 1.186 | 0.006 | 2.471 | 0.016 | 18.1 | 1.1 |
| | 48.344 | 1912.96 | −18.14 | M | 49.2 | 2.2 | 777.3 | 36.0 | 118.9 | 5.6 | 0.063 | 0.004 | 1.198 | 0.002 | 2.491 | 0.005 | 18.9 | 0.1 |
| | 48.354 | 1912.91 | −18.17 | M | 118.0 | 5.3 | 2422.9 | 111.4 | 242.5 | 24.3 | 0.049 | 0.003 | 1.198 | 0.003 | 2.495 | 0.005 | 18.8 | 0.2 |
| | 48.404 | 1912.62 | −15.28 | NM | 84.6 | 3.4 | 1381.0 | 56.8 | 212.9 | 13.4 | 0.061 | 0.004 | 1.196 | 0.003 | 2.490 | 0.007 | 18.9 | 0.2 |
| | 48.414 | 1912.56 | −14.86 | NM | 205.3 | 8.1 | 2660.4 | 107.6 | 491.5 | 20.2 | 0.077 | 0.004 | 1.198 | 0.002 | 2.489 | 0.003 | 18.8 | 0.1 |
| | 48.424 | 1912.50 | −15.13 | NM | 105.2 | 4.1 | 1441.0 | 60.2 | 214.2 | 8.6 | 0.073 | 0.004 | 1.196 | 0.004 | 2.493 | 0.007 | 18.8 | 0.2 |
| | 48.434 | 1912.44 | −15.26 | NM | 60.4 | 2.4 | 878.1 | 37.1 | 118.4 | 5.1 | 0.069 | 0.004 | 1.201 | 0.002 | 2.491 | 0.010 | 18.7 | 0.3 |
| | 48.444 | 1912.39 | −15.45 | NM | 25.3 | 1.0 | 358.7 | 14.6 | 55.1 | 2.7 | 0.071 | 0.004 | 1.196 | 0.002 | 2.489 | 0.005 | 18.9 | 0.1 |
| | 48.454 | 1912.33 | −15.37 | M | 3.9 | 0.2 | 37.8 | 2.0 | −0.8 | 0.7 | 0.103 | 0.007 | 1.176 | 0.005 | 2.472 | 0.011 | 18.3 | 0.6 |
| | 48.464 | 1912.27 | −15.53 | M | 10.7 | 0.4 | 129.2 | 5.4 | 18.1 | 1.6 | 0.083 | 0.005 | 1.194 | 0.003 | 2.484 | 0.005 | 18.6 | 0.3 |
| | 48.474 | 1912.21 | −15.65 | M | 58.5 | 2.3 | 1016.0 | 45.5 | 138.8 | 5.9 | 0.058 | 0.003 | 1.206 | 0.004 | 2.495 | 0.007 | 18.9 | 0.2 |
| | 48.484 | 1912.15 | −16.36 | M | 56.2 | 2.3 | 1075.6 | 48.6 | 95.0 | 4.6 | 0.052 | 0.003 | 1.195 | 0.003 | 2.483 | 0.005 | 18.8 | 0.1 |
| | 48.494 | 1912.10 | −15.65 | M | 66.7 | 2.7 | 1029.0 | 48.6 | 118.7 | 5.9 | 0.065 | 0.004 | 1.195 | 0.004 | 2.480 | 0.008 | 18.6 | 0.3 |
| Ra-79 | 72.159 | 1775.45 | −19.16 | M | 9.1 | 0.4 | 168.9 | 7.2 | 21.7 | 2.8 | 0.054 | 0.003 | 1.211 | 0.007 | 2.496 | 0.010 | 18.7 | 0.4 |
| | 72.169 | 1775.39 | −19.09 | M | 14.1 | 0.6 | 278.5 | 12.3 | 33.3 | 2.4 | 0.051 | 0.003 | 1.204 | 0.003 | 2.506 | 0.009 | 19.1 | 0.3 |
| | 72.179 | 1775.32 | −18.77 | M | 13.4 | 0.6 | 342.6 | 14.5 | 42.3 | 2.9 | 0.039 | 0.002 | 1.201 | 0.005 | 2.509 | 0.006 | 19.1 | 0.5 |
| | 72.189 | 1775.26 | −18.16 | M | 71.6 | 3.0 | 753.4 | 35.2 | 175.9 | 8.6 | 0.095 | 0.006 | 1.199 | 0.004 | 2.508 | 0.010 | 18.7 | 0.5 |
| | 72.199 | 1775.20 | −17.76 | NM | 67.3 | 2.7 | 984.5 | 44.4 | 153.2 | 10.5 | 0.068 | 0.004 | 1.195 | 0.002 | 2.490 | 0.006 | 18.7 | 0.3 |
| | 72.209 | 1775.14 | −17.42 | NM | 94.4 | 3.9 | 1400.6 | 57.7 | 251.4 | 11.3 | 0.067 | 0.004 | 1.204 | 0.002 | 2.494 | 0.004 | 18.9 | 0.1 |
| | 72.219 | 1775.07 | −17.91 | NM | 47.1 | 2.1 | 695.6 | 30.8 | 104.1 | 5.8 | 0.068 | 0.004 | 1.207 | 0.003 | 2.513 | 0.007 | 18.7 | 0.5 |
| | 72.229 | 1775.01 | −17.70 | NM | 34.3 | 1.5 | 828.9 | 35.3 | 121.8 | 6.4 | 0.041 | 0.003 | 1.203 | 0.003 | 2.503 | 0.008 | 18.6 | 0.3 |
| | 72.249 | 1774.87 | −17.78 | M | 10.1 | 0.5 | 220.8 | 9.3 | 29.1 | 2.0 | 0.046 | 0.003 | 1.202 | 0.005 | 2.509 | 0.009 | 18.8 | 0.4 |
| | 72.259 | 1774.80 | | M | 3.7 | 0.2 | 80.4 | 4.7 | 10.2 | 1.9 | 0.046 | 0.004 | 1.197 | 0.006 | 2.494 | 0.016 | 17.7 | 1.0 |
| | 72.269 | 1774.73 | −17.73 | M | 25.1 | 1.0 | 285.1 | 12.3 | 39.1 | 2.6 | 0.088 | 0.005 | 1.205 | 0.002 | 2.495 | 0.007 | 19.0 | 0.2 |
| | 72.329 | 1774.32 | −17.28 | M | 24.9 | 1.0 | 325.2 | 13.7 | 50.4 | 3.1 | 0.076 | 0.004 | 1.197 | 0.003 | 2.491 | 0.005 | 18.9 | 0.3 |
| | 72.339 | 1774.25 | −16.45 | NM | 29.2 | 1.2 | 260.5 | 11.4 | 50.8 | 4.8 | 0.112 | 0.007 | 1.201 | 0.004 | 2.508 | 0.006 | 19.0 | 0.2 |
| | 72.349 | 1774.18 | −17.09 | NM | 18.5 | 0.8 | 222.8 | 9.7 | 36.3 | 2.3 | 0.083 | 0.005 | 1.192 | 0.003 | 2.489 | 0.005 | 18.7 | 0.1 |
| | 72.359 | 1774.11 | −19.69 | NM | 11.0 | 0.5 | 125.2 | 7.8 | 23.8 | 1.5 | 0.088 | 0.007 | 1.213 | 0.003 | 2.511 | 0.005 | 19.0 | 0.4 |
| | 72.369 | 1774.03 | −19.74 | NM | 43.4 | 1.6 | 383.1 | 16.7 | 61.5 | 3.1 | 0.113 | 0.007 | 1.197 | 0.001 | 2.506 | 0.005 | 18.6 | 0.2 |
| | 72.379 | 1773.96 | −19.89 | NM | 80.7 | 3.3 | 1252.5 | 50.5 | 174.9 | 8.8 | 0.064 | 0.004 | 1.200 | 0.003 | 2.499 | 0.004 | 19.0 | 0.2 |
| | 72.389 | 1773.87 | −19.44 | NM | 6.1 | 0.3 | 105.6 | 5.9 | 9.8 | 0.9 | 0.058 | 0.004 | 1.199 | 0.003 | 2.507 | 0.009 | 19.0 | 0.4 |
| | 72.399 | 1773.78 | −19.56 | M | 11.3 | 0.5 | 154.3 | 7.3 | 24.7 | 1.4 | 0.073 | 0.005 | 1.203 | 0.004 | 2.493 | 0.009 | 19.1 | 0.2 |
| | 72.409 | 1773.69 | −21.02 | M | 20.1 | 0.8 | 222.3 | 11.1 | 34.4 | 1.9 | 0.090 | 0.006 | 1.200 | 0.005 | 2.503 | 0.009 | 18.9 | 0.3 |
| | 72.419 | 1773.60 | −21.67 | M | 41.0 | 1.6 | 467.7 | 19.5 | 72.0 | 3.1 | 0.088 | 0.005 | 1.204 | 0.002 | 2.498 | 0.006 | 19.0 | 0.2 |
| | 72.429 | 1773.51 | −22.30 | M | 4.9 | 0.2 | 54.3 | 4.3 | 5.5 | 1.0 | 0.090 | 0.008 | 1.178 | 0.004 | 2.473 | 0.010 | 18.7 | 0.7 |
| | 72.439 | 1773.42 | | NM | 24.1 | 1.1 | 285.2 | 12.5 | 77.6 | 3.9 | 0.084 | 0.005 | 1.214 | 0.006 | 2.494 | 0.008 | 19.1 | 0.3 |
| | 72.451 | 1773.33 | −21.07 | NM | 90.0 | 3.7 | 1378.1 | 59.5 | 204.0 | 8.7 | 0.065 | 0.004 | 1.202 | 0.002 | 2.496 | 0.005 | 19.0 | 0.1 |

Where: 'M' refers to monsoon and 'NM' refers to non-monsoon and; all uncertainties represent 95% confidence intervals.

negative values in spring (e.g. Tian et al., 2003 and references therein). With this expected cycle in mind, the δ¹⁸O compositions of Ra-79 samples are irregular and do not indicate a noticeable recurring annual cycle that might be expected given the approximate two years of accumulation integrated by the core section. In contrast, the 20th century core sections (Ra-51 and Ra-37), which integrate 1.6 years and 8.9 months respectively, show similar variations over time; however given that Ra-37 does not integrate a full year, only limited comparisons between the two records can be made. We note that oxygen isotope compositions are most depleted in the deepest core section (Ra-79), reaching more elevated values (i.e. less negative) in the 20th century ice, which

is similar to the increasing 20th century trend observed by Thompson et al. (2000) and Kaspari et al. (2007).

### 3.1.2. Elemental concentrations

Strong correlations exist between Pb, Ba and In concentrations in all ice core data, with Ba concentrations having been used here as a proxy for mineral dust levels. Although In is enriched in volcanic emissions (e.g. Hinkley et al., 1999), it is also present in crustal material at a concentration of approximately 50 ppb (Taylor and McLennan, 1985). The strong [Pearson] correlation between In and Ba concentrations for all ERG data (R = 0.96) therefore suggests that In present in ERG ice

originates from dust. Similarly, the strong [Pearson] correlation between Pb and Ba concentrations for all data (R = 0.97) and between Pb and In concentrations (R = 0.98) indicates that all measured elemental concentrations in the ERG ice core section record presented here are controlled by inputs of mineral dust.

Elemental Pb/Ba ratios have been used previously to indicate additional inputs of Pb relative to Ba such as from the input of anthropogenic or volcanic Pb (e.g. Vallelonga et al., 2002). Elemental Pb/Ba ratios for Ra-79 show a high degree of variability over time, ranging from 0.04 to 0.11 and averaging ~0.07, compared to an average Pb/Ba ratio in the Earth's upper continental crust of ~0.03 and an average Pb/Ba ratio in Chinese Loess of ~0.04 (ranging from ~0.03 to ~0.05, see McLennan, 2001). Thus many samples in the Ra-79 ice core section are somewhat enriched in Pb. This would traditionally imply inputs of anthropogenic and/or volcanic Pb, however, no evidence has been found for anthropogenic influence in high-altitude Himalayan ice prior to the 20th century (Kaspari et al., 2009b; Lee et al., 2011). Similarly, sulphate concentrations analysed in high-altitude central Himalayan ice do not indicate significant volcanic events that correspond to the timing of the Ra-79 (18th century) ice core (Duan et al., 2007) and elemental In/Pb ratios are comparable to typical values in the upper continental crust (~0.003, McLennan, 2001). Consequently, it is proposed here that variability in Pb/Ba ratios in Ra-79 is associated with a natural variability in inputs of mineral dust.

Applying this line of reasoning to variability in the 20th century Pb/Ba record, only one sample at a depth of 35.470 m, with a Pb/Ba ratio of 0.13, lies marginally outside of the upper two standard deviations of the naturally ranging Ra-79 Pb/Ba data set, suggesting possible Pb enrichment. Since no volcanic events have been recorded in ERG ice at the corresponding time (mid 1952, Xu et al., 2009a), this Pb enrichment could only result from anthropogenic inputs.

### 3.1.3. Lead isotopes

Ra-79 data have been used as an indicator of a 'natural background' that is devoid of contributions from anthropogenic (and volcanic) Pb. With the exception of a sample at 72.429 m, with a $^{206}Pb/^{207}Pb$ ratio of 1.178 ± 0.004 (all uncertainties presented here represent the 95% confidence intervals), Pb isotopic characteristics do not vary considerably within measurement uncertainties, averaging 1.201 ± 0.006, 2.495 ± 0.006, and 18.7 ± 0.2 for the $^{206}Pb/^{207}Pb$, $^{208}Pb/^{207}Pb$ and $^{206}Pb/^{204}Pb$ ratios respectively which is in agreement with the natural background isotopic signature (i.e. prior to 1950) reported by Lee and co-workers (Lee et al. 2011). Whilst the outlying sample at 72.429 m features a markedly less-radiogenic $^{206}Pb/^{207}Pb$ ratio, this sample does not have an unusual Pb/Ba value; consequently we consider it to be influenced by mineral dust of a different origin.

The range of $^{206}Pb/^{207}Pb$ ratios in the 20th century ice core sections (Ra-51 and Ra-37) is similar to that in the 18th century ice core data (Ra-79), however there appears to be a greater number of samples characterised by relatively lower $^{206}Pb/^{207}Pb$ ratios. Traditionally such deviations would be associated with anthropogenic inputs (e.g. the Northern Hemisphere anthropogenic aerosol $^{206}Pb/^{207}Pb$ average is ~1.14, Bollhöfer and Rosman, 2001); however, corresponding 20th century Pb/Ba ratios, with the exception of one sample at 35.470 m (Pb/Ba = 0.13, previously noted in Section 3.1.2), do not deviate outside of the limits of natural variability defined by Ra-79 data. Similarly, this anomalous Pb/Ba ratio at 35.470 m corresponds to a $^{206}Pb/^{207}Pb$ of 1.210 ± 0.002 which lies within natural limits (defined from Ra-79 data) thus eliminating volcanic or anthropogenic Pb inputs.

Consequently, based on Pb/Ba ratios, and Pb isotopes, we see no evidence for the additional input of anthropogenic or volcanic Pb in any of the ice core sections discussed here, indicating atmospheric chemistry to be dominated by mineral dust inputs. The lack of any anthropogenic inputs agrees with recent studies that also demonstrate little to no anthropogenic inputs into the high-altitude Himalayas prior to the 1950s (e.g. Kaspari et al., 2009b; Lee et al., 2011).

In relation to relationships between Pb concentrations and $^{206}Pb/^{207}Pb$ isotopic ratios, 18th century ice core data show respective monsoon and non-monsoon [Pearson] correlations of R = 0.14 and R = −0.17, both of which are weak and imply little correlation between the two parameters. For 20th century ice, the respective correlations for monsoon and non-monsoon ice are R = 0.58 and R = 0.12 for Ra-51 (~1912) and R = 0.69 and R = −0.43 for Ra-37 (~1952). Therefore in both cases, Pb concentrations and $^{206}Pb/^{207}Pb$ ratios show consistent moderate positive correlations during the monsoon season and weakened inconsistent correlations during the non-monsoon season. As anthropogenic and volcanic contributions have been eliminated as a possible source of Pb in the 20th century ice discussed here (see preceding sections), this result implies some association between low monsoon Pb concentrations and inputs from one or more mineral dust sources characterised by less radiogenic Pb isotopic ratios, and vise versa.

### 3.2. Snow pit samples

Lee et al. (2008) have published trace element concentrations and $\delta^{18}O$ values on the same snow pit samples that are discussed here. Oxygen isotopic compositions were discussed by the authors and hence are not discussed here; new Pb, Ba and In concentration data and Pb isotopes are shown in Table 2.

### 3.2.1. Elemental concentrations

Snow pit Pb, Ba and In concentrations are greater than those observed in the ice core samples. The Ba/In [Pearson] correlation is R = 0.98 which implies that In is dominated by mineral dust, as was the case for the ice core samples. In contrast, the Pb/Ba and Pb/In correlations are slightly weaker, R = 0.78 and R = 0.81 respectively, which implies a slight decoupling of the Pb and the mineral dust signal relative to that observed in the ERG ice. Given that volcanic inputs can be excluded (Xu et al., 2009a), this result indicates the input of anthropogenic Pb. Such inputs are further confirmed when considering Pb/Ba elemental ratios, which reach 0.19, relative to a previously defined natural maximum of 0.13, as seen in ice core data.

Using the seasonal allocation (monsoon/non-monsoon) defined by Lee and co-workers, monsoon Pb/Ba ratios range from 0.04 to 0.16 (average: ~0.08) and non-monsoon ratios range from 0.08 to 0.19 (average: ~0.12). These results suggest somewhat increased inputs of anthropogenic Pb during the non-monsoon relative to the monsoon season.

### 3.2.2. Lead isotopes

Snow pit isotopic $^{206}Pb/^{207}Pb$ ratios range from 1.16 to 1.21 compared to the 'natural' range defined from the ice core samples of 1.18–1.21. This slight decrease in isotopic ratios from the natural range is indicative of anthropogenic Pb influences (see Bollhöfer and Rosman, 2001). The moderate to strong negative [Pearson] correlation that exists between Pb/Ba ratios and $^{206}Pb/^{207}Pb$ ratios, R = −0.77 further supports anthropogenic influence.

Monsoon $^{206}Pb/^{207}Pb$ ratios range from 1.16 to 1.21 (average: ~1.19) and non-monsoon ratios range from 1.17 to 1.18 (average: ~1.17). The expanded range in monsoon isotopic ratios suggests the input of impurities from a range of sources, both natural and anthropogenic. However, the average monsoon $^{206}Pb/^{207}Pb$ ratio of ~1.19 suggests that natural inputs of Pb dominate over anthropogenic inputs. In contrast, the range in non-monsoon isotopic ratios is much smaller, indicating the input of impurities from a smaller array of sources, or alternatively from multiple sources of Pb that possess similar isotopic characteristics. Additionally, the average non-monsoon $^{206}Pb/^{207}Pb$ ratio of ~1.17 implies that anthropogenic inputs are more important during non-monsoon times.

**Table 2**
Analysed Mount Everest snow pit data.

| Snow pit samples | δ¹⁸O | Season | Concentrations | | | | | | | | Lead Isotopic Ratios | | | | | |
|---|---|---|---|---|---|---|---|---|---|---|---|---|---|---|---|---|
| Depth (cm) | | | Pb (pg g⁻¹) | ± | Ba (pg g⁻¹) | ± | In (fg g⁻¹) | ± | Pb/Ba | ± | ²⁰⁶Pb/²⁰⁷Pb | ± | ²⁰⁸Pb/²⁰⁷Pb | ± | ²⁰⁶Pb/²⁰⁴Pb | ± |
| 0–5 | −10.1 | M | 78.1 | 3.0 | 720.6 | 28.5 | 118.5 | 4.8 | 0.108 | 0.006 | 1.169 | 0.002 | 2.461 | 0.003 | 18.34 | 0.06 |
| 5–10 | −13.3 | M | 110.1 | 4.4 | 1756.8 | 71.6 | 276.7 | 11.3 | 0.063 | 0.004 | 1.184 | 0.001 | 2.486 | 0.003 | 18.63 | 0.09 |
| 10–15 | −20.2 | M | 6.9 | 0.3 | 51.6 | 2.4 | 9.9 | 0.8 | 0.133 | 0.008 | 1.161 | 0.001 | 2.452 | 0.003 | 18.28 | 0.06 |
| 15–20 | −21.2 | M | 9.7 | 0.4 | 60.9 | 2.7 | 14.3 | 0.7 | 0.160 | 0.010 | 1.167 | 0.002 | 2.462 | 0.003 | 18.27 | 0.09 |
| 20–25 | −20.2 | M | 22.3 | 0.9 | 309.6 | 13.0 | 46.1 | 2.0 | 0.072 | 0.004 | 1.187 | 0.002 | 2.486 | 0.003 | 18.64 | 0.08 |
| 25–30 | −19.0 | M | 20.3 | 0.9 | 214.5 | 9.2 | 46.5 | 2.0 | 0.095 | 0.006 | 1.186 | 0.002 | 2.485 | 0.003 | 18.65 | 0.09 |
| 30–35 | −20.6 | M | 7.0 | 0.3 | 93.7 | 4.0 | 16.1 | 0.9 | 0.075 | 0.004 | 1.183 | 0.002 | 2.485 | 0.003 | 18.68 | 0.07 |
| 35–40 | −22.9 | M | 44.2 | 1.8 | 652.1 | 27.1 | 112.0 | 4.7 | 0.068 | 0.004 | 1.199 | 0.002 | 2.497 | 0.003 | 18.91 | 0.08 |
| 40–45 | −22.5 | M | 48.0 | 4.7 | 861.2 | 115.7 | 123.2 | 13.4 | 0.056 | 0.003 | 1.201 | 0.003 | 2.506 | 0.006 | 18.99 | 0.07 |
| 45–50 | −21.5 | M | 3.9 | 0.2 | 26.0 | 1.2 | 3.5 | 0.5 | 0.152 | 0.010 | 1.176 | 0.002 | 2.472 | 0.005 | 18.61 | 0.08 |
| 50–55 | −23.3 | M | 41.2 | 1.6 | 693.8 | 28.1 | 123.6 | 5.0 | 0.059 | 0.003 | 1.193 | 0.002 | 2.495 | 0.003 | 18.79 | 0.07 |
| 55–60 | −18.4 | M | 215.1 | 8.8 | 5797.3 | 239.3 | 1013.2 | 41.9 | 0.037 | 0.002 | 1.208 | 0.001 | 2.51 | 0.002 | 19.07 | 0.06 |
| 60–65 | −18.3 | M | 39.0 | 1.5 | 608.0 | 24.5 | 103.4 | 4.2 | 0.064 | 0.004 | 1.191 | 0.001 | 2.492 | 0.003 | 18.81 | 0.08 |
| 65–70 | −19.5 | M | 13.0 | 0.5 | 280.1 | 11.1 | 27.5 | 1.3 | 0.046 | 0.003 | 1.189 | 0.002 | 2.493 | 0.003 | 18.75 | 0.08 |
| 70–75 | −20.8 | M | 18.0 | 0.7 | 368.0 | 14.7 | 58.3 | 2.4 | 0.049 | 0.003 | 1.190 | 0.001 | 2.492 | 0.003 | 18.79 | 0.06 |
| 75–80 | −22.7 | M | 19.0 | 0.8 | 191.6 | 8.2 | 36.3 | 1.8 | 0.099 | 0.006 | 1.183 | 0.001 | 2.480 | 0.003 | 18.60 | 0.07 |
| 80–85 | −23.4 | M | 5.6 | 0.2 | 38.3 | 1.7 | 8.0 | 0.6 | 0.146 | 0.009 | 1.177 | 0.002 | 2.473 | 0.003 | 18.56 | 0.07 |
| 85–90 | −22.1 | M | 35.9 | 1.5 | 753.5 | 31.6 | 174.2 | 7.3 | 0.048 | 0.003 | 1.197 | 0.001 | 2.498 | 0.002 | 18.89 | 0.06 |
| 90–95 | −21.2 | M | 22.3 | 0.9 | 198.4 | 8.7 | 42.2 | 1.9 | 0.112 | 0.007 | 1.187 | 0.002 | 2.484 | 0.004 | 18.70 | 0.06 |
| 95–100 | −20.3 | M | 15.7 | 0.7 | 251.3 | 10.7 | 46.9 | 2.0 | 0.062 | 0.004 | 1.196 | 0.001 | 2.498 | 0.002 | 18.85 | 0.06 |
| 100–105 | −19.6 | M | 18.6 | 0.8 | 288.3 | 12.2 | 37.3 | 1.6 | 0.065 | 0.004 | 1.189 | 0.001 | 2.485 | 0.003 | 18.81 | 0.05 |
| 105–110 | −19.9 | M | 17.6 | 0.7 | 221.9 | 8.9 | 72.3 | 2.9 | 0.079 | 0.005 | 1.200 | 0.002 | 2.500 | 0.003 | 18.96 | 0.08 |
| 110–115 | −20.1 | M | 13.3 | 0.5 | 295.7 | 11.5 | 41.4 | 1.8 | 0.045 | 0.002 | 1.196 | 0.002 | 2.497 | 0.003 | 18.97 | 0.07 |
| 115–120 | −18.5 | NM | 346.6 | 13.8 | 2604.0 | 104.8 | 577.7 | 24.6 | 0.133 | 0.008 | 1.176 | 0.001 | 2.466 | 0.003 | 18.34 | 0.06 |
| 120–125 | −17.7 | NM | 309.4 | 12.3 | 2019.3 | 81.5 | 458.8 | 19.7 | 0.153 | 0.009 | 1.172 | 0.002 | 2.459 | 0.003 | 18.38 | 0.07 |
| 125–130 | −17.3 | NM | 63.6 | 2.3 | 368.2 | 14.4 | 100.8 | 3.9 | 0.173 | 0.009 | 1.167 | 0.002 | 2.456 | 0.003 | 18.34 | 0.05 |
| 130–135 | −16.7 | NM | 43.0 | 2.0 | 489.2 | 30.5 | 99.9 | 5.6 | 0.088 | 0.005 | 1.175 | 0.003 | 2.471 | 0.006 | 18.45 | 0.10 |
| 135–140 | −17.5 | NM | 23.7 | 0.9 | 211.6 | 9.3 | 66.2 | 2.8 | 0.112 | 0.007 | 1.174 | 0.002 | 2.473 | 0.004 | 18.50 | 0.09 |
| 140–145 | −17.4 | NM | 17.8 | 0.8 | 202.9 | 8.6 | 35.1 | 1.6 | 0.088 | 0.005 | 1.177 | 0.002 | 2.472 | 0.003 | 18.57 | 0.08 |
| 145–150 | −16.4 | NM | 70.3 | 2.8 | 869.0 | 34.8 | 289.1 | 11.9 | 0.081 | 0.005 | 1.182 | 0.002 | 2.485 | 0.004 | 18.75 | 0.09 |
| 150–155 | −17.0 | NM | 68.0 | 2.8 | 741.5 | 30.4 | 139.7 | 5.9 | 0.092 | 0.005 | 1.175 | 0.002 | 2.467 | 0.003 | 18.50 | 0.05 |
| 155–160 | −17.9 | NM | 26.8 | 1.1 | 186.4 | 8.1 | 47.3 | 2.0 | 0.144 | 0.009 | 1.173 | 0.001 | 2.468 | 0.002 | 18.45 | 0.07 |
| 160–165 | −17.6 | NM | 10.4 | 0.4 | 121.7 | 5.1 | 23.3 | 1.0 | 0.085 | 0.005 | 1.166 | 0.002 | 2.458 | 0.003 | 18.29 | 0.06 |
| 165–170 | −16.9 | NM | 9.3 | 0.4 | 53.8 | 2.5 | 7.2 | 0.8 | 0.172 | 0.011 | 1.170 | 0.001 | 2.468 | 0.003 | 18.38 | 0.06 |
| 170–175 | −15.7 | NM | 18.2 | 0.8 | 96.4 | 4.1 | 17.7 | 0.8 | 0.189 | 0.011 | 1.174 | 0.002 | 2.465 | 0.003 | 18.51 | 0.06 |
| 175–180 | −13.4 | NM | 75.0 | 3.0 | 859.5 | 35.6 | 140.0 | 5.9 | 0.087 | 0.005 | 1.175 | 0.001 | 2.468 | 0.002 | 18.50 | 0.07 |
| 180–185 | −11.9 | NM | 103.4 | 4.1 | 1223.9 | 48.5 | 231.7 | 9.3 | 0.084 | 0.005 | 1.177 | 0.001 | 2.464 | 0.002 | 18.52 | 0.05 |
| 185–190 | −11.4 | NM | 176.9 | 7.2 | 1107.8 | 46.2 | 120.3 | 6.0 | 0.160 | 0.009 | 1.168 | 0.001 | 2.455 | 0.003 | 18.29 | 0.07 |
| 190–195 | −13.3 | NM | 233.0 | 9.5 | 2098.2 | 86.5 | 399.7 | 17.3 | 0.111 | 0.006 | 1.173 | 0.001 | 2.460 | 0.003 | 18.39 | 0.06 |
| 195–200 | −16.3 | NM | 347.3 | 14.0 | 2455.8 | 99.8 | 410.4 | 18.0 | 0.141 | 0.008 | 1.171 | 0.001 | 2.460 | 0.002 | 18.42 | 0.06 |
| 200–205 | −18.2 | NM | 39.7 | 1.6 | 256.6 | 11.1 | 42.5 | 1.9 | 0.155 | 0.009 | 1.172 | 0.002 | 2.460 | 0.003 | 18.37 | 0.07 |
| 205–210 | −18.0 | NM | 34.2 | 1.4 | 289.1 | 13.2 | 40.0 | 2.0 | 0.118 | 0.007 | 1.167 | 0.001 | 2.456 | 0.003 | 18.32 | 0.06 |

Where: Snow pit sample depths, oxygen isotopes and seasonal allocation are from Lee et al. (2008) and remaining data are from this work; 'M' refers to monsoon and 'NM' refers to non-monsoon and; all uncertainties represent 95% confidence intervals.

This conclusion is in agreement with elemental discussions in the previous section. Potential sources of Pb preserved in the snow pit samples are discussed in detail in Section 3.5.

Correlations [Pearson] between Pb concentrations and ²⁰⁶Pb/²⁰⁷Pb isotopic ratios in monsoon and non-monsoon snow pit samples are weak (R = 0.38 and R = 0.04 respectively). This result suggests that inputs of anthropogenic impurities into the ERG region are not strictly linked to elevated levels of Pb, which is in contrast to anthropogenic Pb records preserved in polar ice (e.g. Candelone et al., 1995; Vallelonga et al., 2002).

### 3.3. Seasonal variability in the natural sources of lead in 18th century ice

Isotopic ²⁰⁶Pb/²⁰⁷Pb and elemental ratios of measured 18th century ice core samples showed no evidence for the presence of anthropogenic or volcanic inputs at the sampling site, therefore all Pb present is attributed to mineral dust inputs (see Section 3.1). Therefore all Pb present is attributed to mineral dust inputs. All seasonally differentiated 18th century Pb isotopic data are shown in a three-isotope plot in Fig. 3, along with potential source area (PSA) Pb isotopic data. Data from Lee et al. (2011) corresponding to the period 1205–1792 have been included

for comparison and show good agreement with the new data presented here.

Potential source areas included for comparison have been selected based on a number of criteria: (1) prevailing atmospheric circulations that occur during the monsoon and non-monsoon seasons respectively; (2) highly active dust source regions in the Northern Hemisphere that would be capable of injecting mineral dust into the upper troposphere (see Prospero et al., 2002); (3) the inability of material from Chinese desert regions to be transported southwards (see Section 1); (4) previous studies (see Section 1); and (5) available Pb isotopic data. In regards to the latter, we note that the PSA data that have been utilised for comparison and interpretation are by no means exhaustive. To conclusively interpret the ERG ice core (and snow pit) data presented here, an in-depth investigation and expansion of Pb isotopic data sets corresponding to global dust source regions is required, which goes beyond the scope of the work presented here. We have therefore proceeded with interpretations, but note the limitations that the available PSA Pb isotopic data presents.

As can be seen in Fig. 3, monsoon and non-monsoon isotopic characteristics are generally mixed, with no clear segregation between seasons, indicating complexities in the atmospheric chemistry of the high-altitude Himalayas.
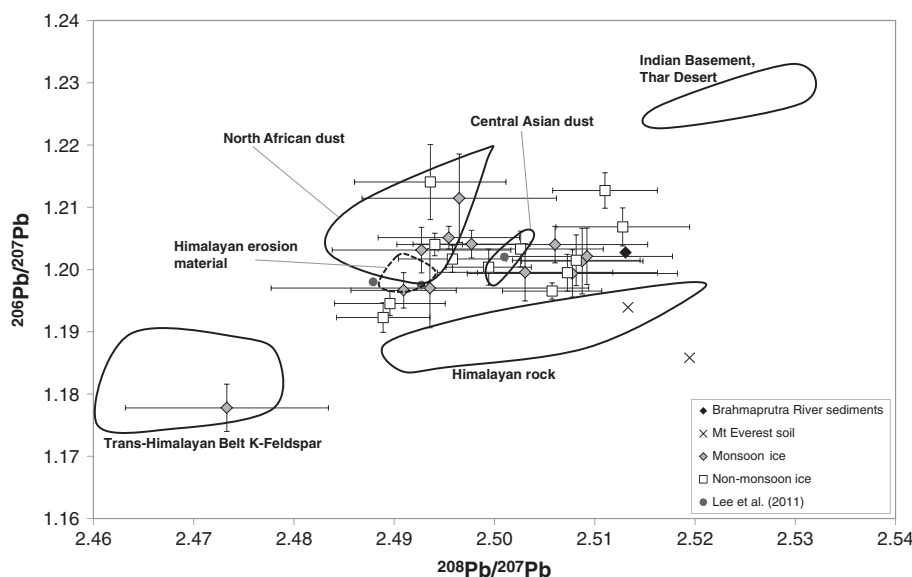
**Fig. 3.** Lead isotopic compositions of 18th century ERG monsoon and non-monsoon ice core samples. Potential dust source areas: Trans-Himalayan Belt (Gariépy et al., 1985); Himalayan rock (Gariépy et al., 1985; Vidal et al., 1992); Himalayan erosion material (Frank and O'Nions, 1998); Brahmaputra River valley sediments (eastern Himalaya) (Millot et al., 2004); Indian Shield basement material (Gariépy et al., 1985); Thar Desert dust (this work); Mt Everest soil (this work); Central Asian (Iran/Pakistan) dust (Staubwasser and Sirocko, 2001); and North African dust (Sun et al., 1980; Vlastelic et al., 2001; Abouchami and Zabel, 2003). Dark grey circles correspond to the ice core data from Lee et al. (2011) dating to 1205–1792.

### 3.3.1. Monsoon

During the monsoon season, atmospheric circulations are dominated by upper-level easterly flow; low-level flow has been described as following easterly and westerly trajectories (Tian et al., 2001; Kaspari et al., 2008). The eastern trajectory is sourced to the Bay of Bengal, with uplift occurring along the valley of the Brahmahputra River. The western trajectory is sourced to the Arabian Sea, with associated air movements across the Indian Peninsula towards the southern slope of the Tibetan Plateau. In both cases, as air masses enter the vicinity of the Himalayas, the topography of the mountain system will guide and channel the masses as they are orographically uplifted to higher altitudes.

With the exception of one outlying less radiogenic data point, all of the monsoon-assigned 18th century ice core data shown in Fig. 3 are consistent with local and regional contributions that could result from monsoonal atmospheric movements, with data grouped in a region defined by local Himalayan sources (rock and erosion material) and Brahmaputra River valley sediments, implying dominant local inputs. Song et al. (2007) have shown that the presence of complex local wind systems in the Rongbuk Valley region could entrain local material closer to the sampling site, which could in turn increase the presence of these inputs relative to longer-range (Indian-derived) material.

There exists one 18th century monsoon sample with distinctly less-radiogenic isotopic characteristics, in agreement with K-Feldspars from the Trans-Himalayan Belt 150 km north of Mount Everest (Gariépy et al., 1985). Ye and Gao (1979) have suggested that monsoon south-westerly winds near the Rongbuk Valley could be distorted by the body of Mount Everest leading to a high frequency of northerly winds at high-altitudes in the region (Y. Song, personal communication, 2009). Additionally, this sample features the most depleted $\delta^{18}O$ value (−22.3‰) reported here, implying intense monsoon activity (Zhang et al., 2005; Kaspari et al., 2007). Stronger winds associated with an intensified monsoon could therefore be capable of transporting larger amounts of northerly material, leading to a stronger relative influence of this material and hence a distinct isotopic signature.

We note in the PSA data that is presented here differing isotopic compositions exist for Himalayan material – "Himalayan erosion material" (Frank and O'Nions, 1998) and "Himalayan rock" (Gariépy et al., 1985; Vidal et al., 1992). These observations demonstrate the variability in the documented isotopic characteristics for the Himalayan region and highlight the need to geographically characterise the Himalayan region for future PSA studies.

### 3.3.2. Non-monsoon

During the non-monsoon period, there is a reversal in atmospheric circulations in the South-East Asian region, resulting in a strong upper tropospheric westerly jet stream that dominates atmospheric circulations across the Asiatic continent, above 700 mbar. Using these non-monsoon atmospheric circulations as a guide to non-monsoon PSAs, we associate 18th century non-monsoon ERG ice core data (shown in Fig. 3) with mixed contributions from: Himalayan material; North African dust; Central Asian dust; and Indian Basement material/Thar Desert dust. These results are consistent with the findings of Lee et al. (2011).

Whilst the majority of the non-monsoon isotopic data cannot be linked to one source, rather a mixture of the aforementioned sources, there exist some distinct data points that demonstrate inputs from local, regional, and long-range sources. Local Himalayan inputs are demonstrated by two data points, distinct from remaining non-monsoon samples, which show the least radiogenic isotopic characteristics of the 18th century non-monsoon ice. This observation additionally supports the year-round presence of local Himalayan wind systems. Two distinct data points that define the upper, radiogenic limits of the non-monsoon data demonstrate regional inputs of Indian-derived material. Given the lack of low-level wind systems that could entrain Indian material during this period, these inputs suggest the injection of Thar Desert dust into the mid to upper troposphere and the subsequent upper westerly transport and deposition of this material at the ERG site (see Shrestha et al., 2000). Finally, the potential for long-range non-monsoon inputs is demonstrated by one distinct data point proximal to North African dust isotopic characteristics. Additionally, agreement of some non-monsoon ice core data with Central Asian isotopic characteristics further supports the influence of long-range mineral dust inputs on the ERG region.
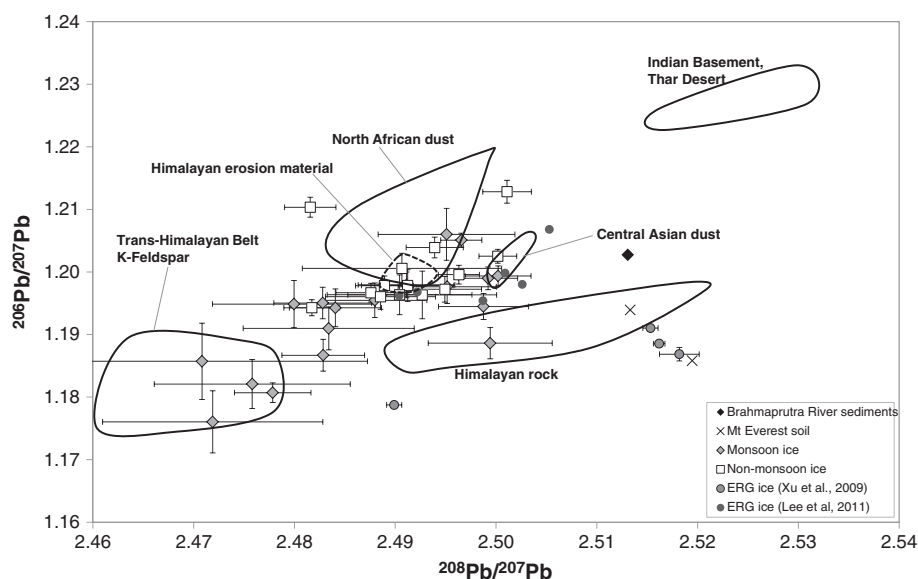
**Fig. 4.** Lead isotopic compositions of 20th century ERG monsoon and non-monsoon samples. See Fig. 3 caption for PSA references. Additionally shown are ERG ice core data from: Xu et al. (2009b) dated to the 20th century and; Lee et al. (2011) dated to the periods 1900–1901 and 1946–1957.

## 3.4. Seasonal variability in the natural sources of lead in 20th century ice

The Pb isotopic characteristics of 20th century monsoon and non-monsoon ERG ice analysed in this study are shown in Fig. 4. As previous studies on the sources of mineral dust reaching the high-altitude Himalayas did not identify changes in the sources of mineral dust over time (e.g. Kaspari et al., 2009a; Lee et al., 2011; Hong et al., 2012), the same PSAs of mineral dust discussed in Section 3.3 have been assumed for the 20th century. Additionally included in Fig. 4 are data from Lee et al. (2011) corresponding to approximately 5 years from the average dates of the 20th century ice cores discussed here and; Pb isotopic data reported by Xu et al. (2009b) on selected ice core samples from a 40 m core, dated to the 20th century, recovered in the ERG region. Relative to the data presented here, Lee and co-workers' data show good agreement; however there are distinct differences in Pb isotope data presented by Xu and co-authors. The ice sampled by Xu and co-workers was recovered only a few metres away from the location of the ERG core discussed here; however given their corresponding isotopic agreement with Mt Everest soil/rock samples from this study, it appears that their samples could be greatly influenced by local rocks and soils, as opposed to sampling atmospheric constituents. In contrast, the ERG data presented here is consistent with isotopic signatures of regional dust sources, and hence longer-range aerosol transport.

The most notable change in the 20th century ice core isotopic systematics, relative to 18th century ice, is a consistent shift toward less-radiogenic isotopic signatures. Given the absence of anthropogenic and volcanic inputs, this transition suggests changes in the relative source strength of identified mineral dust PSAs between the 18th and 20th centuries and/or inputs from one or more unidentified PSAs.

### 3.4.1. Monsoon

Twentieth century monsoon samples show a similar spread in isotopic characteristics compared to 18th century monsoon data suggesting similar PSAs i.e. contributions from Indian derived material and Himalayan material (local and Trans-Himalayan rock, erosional material). However, there appears to be a greater occurrence of samples possessing less radiogenic isotopic signatures that correspond to Trans-Himalayan Belt material, further implying potential inputs into the ERG region from this slightly northerly source. Previously, the occurrence of such inputs (see Section 3.3.1) was linked to distortions in low-

level winds, by the body of Mount Everest, leading to a high frequency of northerly winds at high-altitudes in the ERG region (Ye and Gao, 1979) and possible intense monsoon activity. There is no reason to suggest that such winds could not occur in the 20th century, however ice core data presented here shows that 20th century oxygen isotopes are less negative, suggesting a decrease in the strength of monsoon activity relative to the 18th century. More recently, Zhou et al. (2008) suggested that local wind systems could become dominant in the Rongbuk Valley during break periods in monsoon circulation. If such systems are similarly distorted by the body of Mount Everest, leading to northerly winds, it is possible that this could account for the increased presence of northerly-derived material in the 20th century monsoon ice core data as presented here. In turn this may also indicate an increase in the number of break periods in the summer monsoon during the 20th century.

Further insights into the sources of monsoon mineral dust inputs may also be provided from the moderate positive [Pearson] correlations ($R \approx 0.6$–$0.7$) that exist between 20th century monsoon Pb concentrations and $^{206}Pb/^{207}Pb$ isotopic ratios (see Section 3.1.3). Such correlations suggest that elevated levels of atmospheric dust could be associated with inputs of Himalayan material (rock/erosional material) and/or Indian derived material, both of which are characterised by slightly more radiogenic Pb isotopic ratios, whereas low atmospheric dust levels could be associated with inputs of Trans-Himalayan material from regions slightly to the north of the ERG sampling site, which are characterised by slightly less radiogenic Pb isotopic ratios. Alternatively, the latter may be indicative of a largely background signal, linked to northerly low-level winds, that is otherwise overwhelmed when atmospheric dust levels are high.

We therefore confirm the same PSAs to be influencing the ERG region in the 20th century as in the 18th century, however with increased dominance of dust contributions characterised by less radiogenic Pb isotopic ratios such as from regions to the north of the ERG sampling site.

### 3.4.2. Non-monsoon

Non-monsoon data also show a similar spread in isotopic characteristics compared to 18th century non-monsoon data suggesting the same PSAs (Himalayan rock, Himalayan erosion material, North African dust, Central Asian dust, and Indian Basement/Thar Desert material) to be influencing high-altitude Himalayan atmospheric chemistry in the 20th century. There appears to be a tighter grouping of 20th century

non-monsoon data that is proximal to Himalayan erosion material and North African mineral dust as well as a decrease in the relative influence of Indian-derived material. As aerosol Pb isotopic compositions are not susceptible to environmentally-induced changes (e.g. Sturges and Barrie, 1987), this observation implies that the transition in 20th century isotopic compositions is most likely related to climatic and/or environmental changes. We suggest here three possible scenarios: (1) a decrease in the source strength of Indian-derived material and hence a greater relative influence of Himalayan erosion material and/or North African dust contributions; (2) an increase in the source strength of Himalayan erosion material and/or North African dust; or (3) a combination of (1) and (2).

In the case of (1), Pant and Hingane (1988) reported the mean annual rainfall over north-western India to have largely increased during the 20th century which could lead to greater vegetation cover and land surface stabilisation and hence could decrease the strength of the Thar Desert (Indian) dust source. In the case of (2), Mayewski and Jeschke (1979) have suggested that, on a broad regional scale, glaciers in the Himalayas and Trans-Himalayas have been in a general state of retreat since 1850; increased regions of exposed rock surfaces from this glacier retreat could then in turn act to increase the source strength of local material. In the case of North African sourced mineral dust, Prospero and Lamb (2003) have suggested the African mineral dust source to have been weaker during much of the 20th century before the 1970s, therefore there is no evidence to suggest that the North African dust source itself has been stronger in the 20th century time periods investigated here.

Therefore whilst climate and environmental change in the Himalayas and India may be the most plausible cause of the transition in ice core Pb isotopic data, particularly based on their close proximity to the sampling site, it is clear that no robust conclusions can be made here. To do so, further in-depth investigations on the impact of climate and environmental change on atmospheric transport routes, source strengths, source compositions and post-depositional geochemical processes in the region are needed, which goes beyond the scope of the work presented here.

### 3.5. Seasonal variability in the sources of snow pit lead

Seasonally differentiated snow pit data have been shown in a three isotope plot in Fig. 5, along with the Pb isotopic characteristics of mineral dust PSAs identified in Section 3.4 and a suite of anthropogenic PSAs. Data from Lee et al. (2011) corresponding to 2000–2002 have been included for comparison and show good agreement with the data presented here. It is clearly evident from this comparison that high resolution sampling of Himalayan snow/ice is capable of providing more information on the sources of atmospheric impurities reaching the high-altitude Himalayas, than would otherwise be obtained from whole core integration.

#### 3.5.1. Monsoon

Monsoon samples lie on a mixing line defined by natural, more-radiogenic Pb isotopic characteristics at the upper limits and anthropogenic, less-radiogenic isotopic characteristics at the lower limits. The data has a predominantly radiogenic signature, implying a larger relative natural input of local (Himalayan, Trans-Himalayan Belt) material in the monsoon period. Additionally, the average Pb/Ba ratios for the corresponding samples, whilst elevated, only average 0.13, which is comparable to natural background ratios identified in ice core data.

At the lower limits of the monsoon data set there exist three monsoon samples with less radiogenic isotopic characteristics compared to the bulk of the data set and which possess Pb/Ba ratios of 0.11, 0.13 and 0.16. The latter ratio lies outside of the natural elemental ratio upper limit (0.13, defined in Section 3.1.2), thereby confirming anthropogenic contributions. The former two values are within the natural elemental ratio limit, although the deviation in corresponding isotopic characteristics, away from identified natural PSAs, is most likely indicative of anthropogenic influence.

Specific PSA identification based on isotopic characteristics alone is complicated by the fact that many of the anthropogenic PSA aerosol
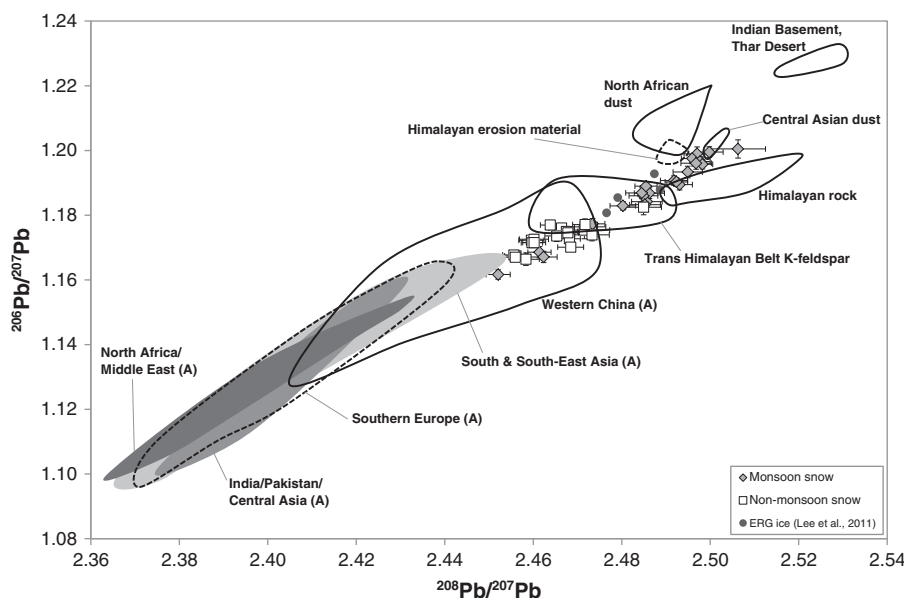


**Fig. 5.** Lead isotopic compositions of ERG snow pit samples dated to 2004/05. See Fig. 3 caption for natural PSA references. Anthropogenic (A) PSA aerosols: China (Mukai et al., 1993, 2001; Wang et al., 2002; Zheng et al., 2004); Central Asia, India and Pakistan (Mukai et al., 1993; Sangster et al., 2000; Bollhöfer and Rosman, 2001); South and South-East Asia (Vietnam, Thailand, Malaysia, Indonesia, Mukai et al., 1993, 2001; Bollhöfer and Rosman, 2000); Southern Europe and North Africa (Bollhöfer and Rosman, 2001). Dark grey circles correspond to ice core data from Lee et al. (2011) dated to the period 2000–2002.

data sets display very similar isotopic characteristics, yet represent geographically different sources. As an initial filter, we have excluded Indonesia and long-range European/North African/Middle East contributions, given atmospheric circulations do not support the transport of aerosols from these regions to the high-altitude Himalayas, during monsoon times. Therefore, monsoon snow pit data presented here are most proximal to the isotopic characteristics of anthropogenic aerosols from Western China, South/South-East Asia, India/Pakistan and/or, Central Asia, which is in agreement with work discussed by Lee et al. (2008, 2011). Based on back trajectory analyses (Ming et al., 2008; Wang et al., 2008; Cong et al., 2009 and references therein) and historical statistical data on industrial activity in these regions (Mitchell, 2007b), we suggest the most important of these source regions to be India and South/South East Asia.

Assuming constant anthropogenic Pb sources, the data presented here suggests that specific atmospheric conditions are required to deposit anthropogenic impurities at the sampling site, and these are sporadic. It is possible that these conditions are associated with a reduction in mineral dust loading, thereby increasing the relative influence of the anthropogenic signal, as was suggested by Lee et al. (2008). Indeed the [Pearson] correlation between Ba concentrations and $^{206}Pb/^{207}Pb$ ratios for snow pit monsoon data is positive, hence supporting this process, however it is only weak to moderate (R = 0.46). We therefore suggest that the monsoon transport of anthropogenic aerosols to the high-altitude Himalayas most likely requires a combination of specific atmospheric transport paths, with reduced mineral dust loading.

### 3.5.2. Non-monsoon

With the exception of one data point, all non-monsoon data display isotopic characteristics that are less radiogenic than natural mineral dust PSAs and most monsoon data. This implies a greater relative input of anthropogenic aerosols during non-monsoon times which is consistent with established findings (Cong et al., 2009; Duan et al., 2009; Kaspari et al., 2011). This does not discount the presence of mineral dust inputs during this season, and based on the mixing line in Fig. 5 it is evident that mineral dust sources discussed in Section 3.4.2 are still active.

Assuming South/South-East Asia and China to be unlikely PSAs based on atmospheric transport paths during non-monsoon times, the Pb isotopic data presented here show agreement with long-range (Southern Europe, North Africa, Middle East) and regional (Central Asia, India) anthropogenic PSAs, in accordance with mineral dust provenance studies. When looking at the historical industrial activity statistics for these regions (Mitchell, 2007a,b), whilst industrial activity in Europe exceeded that for the remaining anthropogenic PSAs in the very late 20th century, this source is also long-range and therefore atmospheric impurity loading would diminish en route to the Himalayas. Similarly, North African industrial activity was greater than that for India and surrounds in the very late 20th century, however the long distance from this source to the ERG region would likely diminish its contribution to deposition on the glacier. Consequently, based on these historical statistics of industrial activity and documented back trajectory analyses (Ming et al., 2008; Cong et al., 2009, 2010; Xu et al., 2010) we further refine the most likely non-monsoon anthropogenic PSAs to be India and Central Asia. This finding is consistent with the findings of Lee et al. (2011), who suggested industrial activity in South Asia (encompassing India as well as the possibility of Bangladesh and Nepal) as the primary source of anthropogenic Pb deposited at the ERG sampling site.

The results presented here emphasise the value of investigating sources of atmospheric chemistry at high resolution. Considering all measured snow pit data as a whole, it is clear from Fig. 5, and annual atmospheric circulations impacting on the high-altitude Himalayan region, that Southern Europe/North Africa, Western China, Central Asia, India and South/South-East Asia could all be PSAs for anthropogenic aerosols for non-seasonally differentiated snow-pit data. However, when assessing data on a seasonal basis and considering corresponding atmospheric circulations, some PSAs can be eliminated thereby allowing further discrimination of the potential sources.

## 4. Conclusions

Three sections from the 2002 East Rongbuk Glacier (ERG) ice core dated to the 18th and 20th centuries and sampled at high spatial resolution and a set of snow pit samples recovered from the ERG site in 2005 have been analysed for Pb, Ba and In concentrations, and Pb isotopes. The data have been used to investigate seasonal variability in the sources of natural and anthropogenic impurities impacting on the ERG environment.

All seasonally segregated ice core data have been shown to be free of anthropogenic and volcanic contributions and hence are indicative of natural inputs of mineral dust into the ERG region. Based on observed ice core isotopic characteristics and prevailing atmospheric transport patterns, we propose 18th century monsoon atmospheric chemistry to be controlled by inputs of local material from the Brahmaputra River valley and other local Himalayan sources, that are likely facilitated by en route entrainment and channelling of monsoonal air masses in the vicinity of the complex Himalayan topography. Eighteenth century non-monsoon data similarly indicate the input of local Himalayan material, implying the year round influence of local winds. Additional non-monsoon inputs of regional (Indian) material and long-range (North African) material are also demonstrated during this period, both of which would be facilitated by the strong upper westerly atmospheric flows that dominate during non-monsoon periods and extend across the Asiatic continent as far west as Africa. We propose the same potential source areas (PSAs) to be impacting on the ERG atmospheric environment during the 20th century, however with a shift in relative source strengths of these PSAs potentially as a result of local (Himalayan) and regional (Indian) climatic and/or environmental change.

Snow pit elemental and isotopic data support inputs of mineral dust and anthropogenic aerosols during both the monsoon and non-monsoon seasons. Monsoon data are dominated by more radiogenic signatures, indicative of larger relative inputs of local (Himalayan, Trans-Himalayan Belt) mineral dust during this period. However, the presence of a few data points possessing less-radiogenic characteristics indicates that small inputs of anthropogenic aerosols are also impacting on the ERG environment. Based on PSA isotopic characteristics, monsoonal atmospheric pathways, back trajectories and industrial historical statistics, these anthropogenic contributions are associated with inputs from India and South Asia. Non-monsoon data are distinctly less radiogenic than both natural mineral dust PSAs and monsoon data, and are therefore indicative of stronger relative inputs of anthropogenic aerosols. We propose India and Central Asia to be the most likely source regions for these inputs, based on PSA isotopic characteristics, atmospheric pathways, back trajectories, and historical statistics.

Whilst the study presented here provides new insights into the sources of both natural mineral dust and anthropogenic pollution reaching the high-altitude Himalayas on a seasonal scale, it is clear that further research is required. Such studies should focus on the Pb isotopic characterisation of a much larger array of natural PSAs, in addition to in-depth investigations of climatic and environmental processes that might lead to transitions in high-altitude Himalayan atmospheric chemistry between the 18th and the 20th centuries. A greater understanding of these factors could more conclusively characterise past high-altitude Himalayan atmospheric chemistry and aid in assessing future change.

## Appendix A. Supplementary data

Supplementary data to this article can be found online at http://dx.doi.org/10.1016/j.scitotenv.2014.03.120.

## References

Abouchami W, Zabel M. Climate forcing of the Pb isotope record of terrigenous input into the Equatorial Atlantic. Earth Planet Sci Lett 2003;213:221–34.

Barry RG. Case studies: the Himalaya (B). Mountain weather and climate. New York: Methuen Co. Ltd; 1981. p. 240–7.

Bollhöfer A, Rosman kJR. Isotopic source signatures for atmospheric lead: the southern hemisphere. Geochim Cosmochim Acta 2000;64:3251–62.

Bollhöfer A, Rosman kJR. Isotopic source signatures for atmospheric lead: the Northern Hemisphere. Geochim Cosmochim Acta 2001;65:1727–40.

Burn LJ, Rosman KJR, Candelone J-P, Vallelonga PT, Burton GR, Smith AM, et al. An ultra-clean technique for accurately analysing Pb isotopes and heavy metals at high spatial resolution in ice cores with sub-pg g$^{-1}$ Pb concentrations. Anal Chim Acta 2009;634:228–36.

Burn-Nunes LJ, Vallelonga P, Loss RD, Burton GR, Moy A, Curran M, et al. Seasonal variability in the input of lead, barium and indium at Law Dome, Antarctica. Geochim Cosmochim Acta 2011;75:1–20.

Burton GR, Rosman KJR, Candelone JP, Burn L, Boutron CF, Hong S. The impact of climatic conditions on Pb and Sr isotopic ratios found in Greenland ice, 7–150 ky BP. Earth Planet Sci Lett 2007;259:557–66.

Candelone JP, Hong S, Pellone C, Boutron CF. Post-Industrial revolution changes in large-scale atmospheric pollution of the Northern Hemisphere by heavy metals as documented in central Greenland snow and ice. J Geophys Res 1995;100:16,605–16.

Chisholm W, Rosman KJR, Boutron CF, Candelone JP, Hong S. Determination of lead isotopic ratios in Greenland and Antarctic snow and ice at picogram per gram concentrations. Anal Chim Acta 1995;311:141–51.

Cong Z, Kang S, Qin D. Seasonal features of aerosol particles recorded in snow from Mt. Qomolangma (Everest) and their environmental implications. J Environ Sci 2009;21:914–9.

Cong Z, Kang S, Dong S, Liu X, Qin D. Elemental and individual particle analysis of atmospheric aerosols from high Himalayas. Environ Monit Assess 2010;160:323–35.

Duan K, Thompson LG, Yao T, Davis ME, Mosley-Thompson E. A 1000 year history of atmospheric sulfate concentrations in southern Asia as recorded by a Himalayan ice core. Geophys Res Lett 2007;34.

Duan K, Wang L, Ren J, Li L, Han J. Seasonal variations in heavy metals concentrations in Mt. Qomolangma Region snow. J Geogr Sci 2009;19:249–56.

Frank M, O'Nions RK. Sources of Pb for Indian Ocean ferromanganese crusts: a record of Himalayan erosion? Earth Planet Sci Lett 1998;158:121–30.

Gariépy C, Allegre CJ, Xu RH. The Pb-isotope geochemistry of granitoids from the Himalaya–Tibet collision zone: implications for crustal evolution. Earth Planet Sci Lett 1985;74:220–34.

Hinkley T, Matsumoto A. Mid-Holocene change in types of degassing volcanoes, using indium in Antarctic ice as a tracer of volcanic source type. Geophys Res Lett 2007;34: L17710.

Hinkley TK, Lamothe PJ, Wilson SA, Finnegan DL, Gerlacg TM. Metal emissions from Kilauea, and a suggested revision of the estimated worldwide metal output by quiescent degassing of volcanoes. Earth Planet Sci Lett 1999;179:315–25.

Hong S, Lee K, Hur SD, Hou S, Burn-Nunes LJ, Boutron CF. Ice core record variations of atmospheric Cu, Zn, Cd, Pb, and Pb isotopes during the past 800 years in Mount Everest. Heavy metals in the environment: selected pages from the ICHMET-15 Conference. Maralte; 2012. p. 345–57.

Hou S, Chappellaz J, Jouzel J, Chu PC, Masson-Delmotte V, Qin D, et al. Summer temperature trend over the past two millennia using air content in Himalayan ice. Clim Past 2007;3:89–95.

Jimi SI, Rosman KJR, Hong S, Candelone JP, Burn LJ, Boutron CF. Simultaneous determination of picogram per gram concentrations of Ba, Pb and Pb isotopes in Greenland ice by thermal ionisation mass spectrometry. Anal Bioanal Chem 2008;390:495–501.

Kang S, Wake CP, Qin D, Mayewski PA, Yao T. Monsoon and dust signals recorded in Dasuopu Glacier, Tibetan Plateau. J Glaciol 2000;46:222–6.

Kang S, Qin D, Mayewski PA, Wake CP, Ren J. Climatic and environmental records from the Far East Rongbuk ice core, Mt Qomolangma (Mt. Everest). Episodes 2001;24: 176–81.

Kang S, Kreutz KJ, Mayewski PA, Qin D, Yao T. Stable-isotopic composition of precipitation over the northern slope of the central Himalaya. J Glaciol 2002;48:519–26.

Kang S, Mayewski PA, Qin D, Sneed SA, Ren J, Zhang D. Seasonal differences in snow chemistry from the vicinity of Mt. Everest, central Himalayas. Atmos Environ 2004; 38:2819–29.

Kang S, Zhang Q, Kaspari S, Qin D, Cong Z, Ren J, et al. Spatial and seasonal variations of elemental composition in Mt. Everest (Qomolangma) snow/firn. Atmos Environ 2007;41:7208–18.

Kaspari S, Mayewski P, Kang S, Sneed S, Hou S, Hooke R, et al. Reduction in northward incursions of the South Asian monsoon since 1400 AD inferred from a Mt. Everest ice core. Geophys Res Lett 2007;34:L16701.

Kaspari S, Hooke RL, Mayewski PA, Kang S, Hou S, Qin D. Snow accumulation rate on Qomolangma (Mount Everest), Himalaya: synchronicity with sites across the Tibetan Plateau on 50–100 year timescales. J Glaciol 2008;54:343–52.

Kaspari S, Mayewski PA, Handley M, Kang S, Hou S, Sneed S, et al. A high-resolution record of atmospheric dust composition and varaibility since A.D. 1650 from a Mount Everest ice core. J Climate 2009a;22:3910–25.

Kaspari S, Mayewski PA, Handley M, Osterberg E, Kang S, Sneed S, et al. Recent increases in atmospheric concentrations of Bi, U, Cs, S and Ca from a 350-year Mount Everest ice core record. J Geophys Res 2009b;114.

Kaspari S, Schwikowski M, Gysel M, Flanner MG, Kang S, Hou S, et al. Recent increase in black carbon concentrations from a Mt. Everest ice core spanning 1860–2000 AD. Geophys Res Lett 2011;38.

Lee K, Hur SD, Hou S, Hong S, Qin X, Ren J, et al. Atmospheric pollution for trace metals in remote high-altitude atmosphere in central Asia as recorded in snow from Mt. Qomolangma (Everest) of the Himalayas. Sci Total Environ 2008;404: 171–81.

Lee K, Hur SD, Hou S, Burn-Nunes LJ, Hong S, Barbante C, et al. Isotopic signatures for natural versus anthropogenic Pb in high-altitude Mt. Everest ice cores during the past 800 years. Sci Total Environ 2011;412:194–202.

Liu Y, Geng Z, Hou S. Spatial and seasonal variation of major ions in Himalayan snow and ice: a source consideration. J Asian Earth Sci 2010;37:195–205.

Matsumoto A, Hinkley TK. Determination of lead, cadmium, indium, thallium and silver in ancient ices from Antarctica by isotope dilution-thermal ionization mass spectrometry. Geochem J 1997;31:175–81.

Mayewski PA, Jeschke PA. Himalayan and Trans-Himalayan glacier fluctuations since AD 1812. Arctic Alpine Res 1979;11:267–87.

McLennan SM. Relationships between the trace element composition of sedimentary rocks and upper continental crust. Geochem. Geophys. Geosyst. 2001;2.

Millot R, Allègre CJ, Gaillardet J, Roy S. Lead isotopic systematics of major river sediments: a new estimate of the Pb isotopic composition of the upper continental crust. Chem Geol 2004;203:75–90.

Ming J, Zhang D, Kang S, Tian W. Aerosol and fresh snow chemistry in the East Rongbuk Glacier on the northern slope of Mt. Qomolangma (Everest). J Geophys Res 2007;112.

Ming J, Cachier H, Xiao C, Qin D, Kang S, Hou S, et al. Black carbon record based on a shallow Himalayan ice core and its climatic implications. Atmos Chem Phys 2008;8: 1343–52.

Mitchell BR. Industry. International historical statistics: Europe 1750–2005. Sixth ed. Hampshire: Palgrave Macmillan; 2007a. p. 455–616.

Mitchell BR. Industry. International historical statistics: Africa, Asia and Oceania 1750–2005. Fifth ed. Hampshire: Palgrave Macmillan; 2007b. p. 363–536.

Mukai H, Furata N, Fujii T, Ambe Y, Sakamoto K, Hashimoto Y. Characterization of sources of lead in the urban air of Asia using ratios of stable lead isotopes. Environ Sci Tech 1993;27:1347–56.

Mukai H, Tanaka A, Fujii T, Zeng Y, Hong Y, Tang J, et al. Regional characteristics of sulpher and lead isotope ratios in the atmosphere at several Chinese urban sites. Environ Sci Tech 2001;35:1064–71.

Pant GB, Hingane LS. Climatic changes in and around the Rajasthan Desert during the 20th century. J Climatol 1988;8:391–401.

Patterson CC, Settle DM. Review of data on eolian fluxes of industrial and natural lead to the lands and seas in remote regions on a global scale. Mar Chem 1987;22: 137–62.

Prospero JM, Lamb PJ. African droughts and dust transport to the Caribbean: climate change implications. Science 2003;302:1024–7.

Prospero JM, Ginoux P, Torres O, Nicholson SE, Gill TE. Environmental characterization of global sources of atmospheric soil dust identified with the Nimbus 7 Total Ozone Mapping Spectrometer (TOMS) absorbing aerosol product. Rev Geophys 2002;40: 2-1–2-31.

Rosman KJR, Ly CV, Van de Velde KP, Boutron CF. A two century record of lead isotopes in high altitude alpine snow and ice. Earth Planet Sci Lett 2000;176:413–24.

Sangster DF, Outridge PM, Davis WJ. Stable lead isotope characteristics of lead ore deposits of environmental significance. Environ Rev 2000;8:115–47.

Shrestha AB, Wake CP, Dibb JE, Mayewski PA, Whitlow SI, Carmichael GR, et al. Seasonal variations in aerosol concentrations and compositions in the Nepal Himalaya. Atmos. Environ. 2000;34:3349–63.

Song Y, Zhu T, Cai X, Lin W, Kang L. Glacier winds in the Rongbuk Valley, north of Mount Everest: 1. Meteorological modeling with remote sensing data. J Geophys Res 2007; 112.

Staubwasser M, Sirocko F. On the formation of laminated sediments on the continental margin off Pakistan: the effects of sediment provenance and sediment redistribution. Mar Geol 2001;172:43–56.

Sturges WT, Barrie LA. Lead 206/207 isotope ratios in the atmosphere of North America as tracers of US and Canadian emissions. Nature 1987;329:144–6.

Sun SS. Lead isotopic study of young volcanic rocks from mid-ocean ridges, ocean islands and islands arcs. Philos Trans R Soc London 1980;297:409–45.

Sun J, Zhang M, Liu T. Spatial and temporal characteristics of dust storms in China and its surrounding regions, 1960–1999: relations to source area and climate. J Geophys Res 2001;106:10,325–33.

Taylor SR, McLennan SM. The continental crust: Its composition and evolution. Oxford: Blackwell Scientific Publications; 1985.

Thompson LG, Yao T, Mosley-Thompson EM, Davis ME, Henderson KA, Lin P-N. A high-resolution millennial record of the South Asian monsoon from Himalayan ice cores. Science 2000;289:1916–9.

Tian L, Masson-Delmotte V, Stievenard M, Yao T, Jouzel J. Tibetan Plateau summer monsoon northward extent revealed by measurements of water stable isotopes. J Geophys Res 2001;106:28,081–8.

Tian L, Yao T, Schuster PF, White JWC, Ichiyanagi K, Pendal E, et al. Oxygen-18 concentrations in recent precipitation and ice cores on the Tibetan Plateau. J Geophys Res 2003; 108:4293. http://dx.doi.org/10.1029/2002JD002173.

Tsai F, Chen GT-J, Liu T-H, Lin W-D, Tu J-Y. Characterizing the transport pathways of Asian dust. J Geophys Res 2008;113.

Vallelonga P, Van de Velde K, Candelone JP, Morgan VI, Boutron CF, Rosman KJR. The lead pollution history of Law Dome, Antarctica, from isotopic measurements on ice cores: 1500 AD to 1989 AD. Earth Planet Sci Lett 2002;204:291–306.

Vidal P, Cocherie A, Le Fort P. Geochemical investigations of the origin of the Manaslu leucogranite (Himalaya, Nepal). Geochim. Cosmochim. Acta 1992;46:2279–92.

Vlastelic I, Abouchami W, Galer SJG, Hofmann AW. Geographic control on Pb isotope distribution and sources in Indian Ocean Fe-Mn deposits. Geochim Cosmochim Acta 2001;65:4303–19.

Wake C, Stievenard M. The amount effect and oxygen isotope ratios recorded in Himalayan snow. Paleoclimate and environmental variability in Austral-Asian transect during the past 2000 years. Japan: Nagoya University; 1995 [November 28-December 1].

Wang W, Liu X, Lu Y, Guo D, Li Y, Tian X, et al. Determination of isotope abundance ratio of lead in Beijing atmospheric aerosol and lead source study. J Chin Mass Spectrom Soc 2002;2002:23.

Wang X, Xu B, Kang S, Cong Z, Yao T. The historical residue trends of DDT, hexachlorocyclohexanes and polycyclic aromatic hydrocarbons in an ice core from Mt. Everest, central Himalayas, China. Atmos Environ 2008;42:6699–709.

Wong GJ, Hawley RL, Lutz ER, Osterberg EC. Trace-element and physical response to melt percolation in Summit (Greenland) snow. Ann Glaciol 2013;54:52–62.

Xu J, Kaspari S, Hou S, Kang S, Qin D, Ren J, et al. Records of volcanic events since AD 1800 in the East Rongbuk ice core from Mt. Qomolangma. Chin Sci Bull 2009a;54:1411–6.

Xu J, Hou S, Chen F, Ren J, Qin D. Tracing the sources of particles in the East Rongbuk ice core from Mt. Qomolangma. Chin Sci Bull 2009b;54:1781–5.

Xu J, Hou S, Qin D, Kaspari S, Mayewski PA, Petit JR, et al. A 108.83-m ice-core record of atmospheric dust deposition at Mt. Qomolangma (Everest), Central Himalaya. Quat Res 2010;73:33–8.

Ye D, Gao Y. Meteorology of the Qinghai–Xizang (Tibet) Plateau (in Chinese). Beijing: Science Press; 1979.

Zhang D, Qin D, Hou S, Kang S, Ren J, Mayewski PA. Climatic significance of $\delta^{18}O$ records from an 80.36 m ice core in the East Rongbuk Glacier, Mount Qomolangma (Everest). Sci China Ser D 2005;48:266–72.

Zhang Q, Kang S, Cong Z, Hou S, Liu Y. Elemental composition in surface snow from the ultra-high elevation area of Mt. Qomolangma (Everest). Chin Sci Bull 2008;53: 289–94.

Zhang Q, Kang S, Kaspari S, Li C, Qin D, Mayewski PA, et al. Rare earth elements in an ice core from Mt. Everest: seasonal variations and potential sources. Atmos Res 2009;94: 300–12.

Zheng J, Tan M, Shibata Y, Tanaka A, Li Y, Zhang G, et al. Characteristics of lead isotope ratios and elemental concentrations in PM10 fraction of airborne particulate matter in Shanghai after the phase-out of leaded gasoline. Atmos Environ 2004;38:1191–200.

Zhou L, Zou H, Shupo M, Li P. Study on impact of the South Asian summer monsoon on the down-valley wind on the northern slope of Mt. Everest. Geophys Res Lett 2008; 35.